A Neural network enhanced hidden Markov model for tourism demand forecasting

A Neural network enhanced hidden Markov model for tourism demand forecasting

Yuan Yao
Institute of Management Science and Engineering,
Business School, Henan University, 475004,
Jinming District, Kaifeng, Henan Province, China
prof.yuanyao@gmail.com

Yi Cao
Management Science and Business Economics Group,
Business School,
University of Edinburgh,
29 Buccleuch Place,
Edinburgh EH8 9JS, UK
jason.caoyi@gmail.com

Abstract

In recent years, tourism demand forecasting has attracted more interests not only in tourism area but in data science field. In this study, we follow the previous relevant data science literatures and propose a new neural network enhanced hidden Markovian structural time series model (NehM-STSM). This model takes a multiplicative error structure of a trend and a seasonal element. The trend is modelled by an artificial neural network while the seasonal element is captured by a tailor-made hidden Markovian model with four components: a persistence replicative cycle, a jump component capturing an unexpected event, an amplitude component reflecting the event strength and a random error term. The empirical research is conducted using US incoming tourism data from twelve major source countries across January 1996-September 2017. The proposed NehM-STSM achieves a better performance than the chosen benchmark models for two error measures and most forecasting horizons.

Keywords: autoregressive neural network; hidden Markovian model; low-pass filter; forecasting

1. Introduction

A major aspect of the tourism industry with significant implications for local community tourism is the fact that tourism flows are seasonal in nature. A close correlation exists between this seasonality and local community decision-making regarding macroeconomic, operation and resource organisation. Precise forecasting of tourism demand for a destination is an important and challenging problem for both the tourism

industry and the local economies as well. Several authors have provided an in-depth analysis of the favourable and unfavourable aspects of seasonality for the local community, such as the work of [1, 2, 3, 4, 5]. Thus, one aspect of seasonality is beneficial due to that the periods with low tourism flows help to restore the natural and municipal resources, whereas it is detrimental because excessive tourist demand and consumption impose enormous strain on resources and infrastructure during periods of high tourism flows, which could create difficulties for local authorities in terms of investment management and workforce recruitment, disrupting the stability of community economics [1, 3, 6]. Therefore, researchers, industry workers and local authorities in charge of decision-making can all benefit from precise forecasting of tourist demand on various resources.

The development, investigation, implementation and assessment of traditional models of statistical forecasting have been undertaken in previous decades in tourism area. These models can be divided into three major categories, namely, deterministic seasonality, stochastic seasonality and multivariate time series models [3]. The assumption underpinning the deterministic seasonality model is that there is an unconditional mean that may fluctuate from season to season over the long term. To obtain a seasonally adjusted series, Lim and McAleer employ moving average (MA) for extracting the seasonal element from the demand series [2]. MA method assumes a constant seasonal pattern over time, which, however, usually evolves over time. Hence the study concludes the inappropriateness of the assumption of constant seasonal patterns over time [2]. Meanwhile, the latest research on tourism demand forecasting has made extensive use of stochastic seasonality models. These models are subdivided into stochastic stationary seasonality model adopting the premise that seasonal pattern is constant [7, 8, 9] and stochastic non-stationary seasonality model underpinned by the premise that seasonal pattern fluctuates [2, 10]. The stochastic non-stationary model has enjoyed broad popularity recently and is distinguished into the seasonal autoregressive integrated moving average (SARIMA) group of seasonal unit root models [11, 12, 13] and the structural time series model (STSM) [14]. The assumption underpinning both model subtypes is that, in addition to trend and seasonal elements, irregular terms are incorporated in tourist arrival data as well. The SARIMA model differentiates between seasonal and non-seasonal elements for stability, while the STSM model implicitly breaks down the time series into two parts: stochastic trend and seasonal with irregular terms. In relation to forecasting of tourism demand, the predominant model employed is the SARIMA model, yet the STSM model has been indicated to consistently have a better performance not only compared to the majority of other similar models, such as naïve Bayesian, neural network and exponential smoothing models [15], but also compared to the SARIMA model [10, 12].

Despite being recently implemented for incoming tourism forecasting, machine learning and methods in operational research areas have been deficiently researched in relation to this field. The artificial neural network (ANN) is applied in forecasting tourism demand of a number of different destinations with other

macroeconomic variables, such as tourism service, hotel information, foreign exchange rate and market expenses, such as the work of [16, 17]. Comparison studies of forecasting tourist visiting a destination via different models usually show the outperformance of machine learning model against the traditional econometric models, such as the work of [15, 18].

On the other hand, some studies claim that the machine learning models, such as the ANN, show the poorest performance in predicting the inflow of tourists from different source countries in the comparison to traditional econometrics models. Such claim is usually due to the under-fitting of the ANN model through an over-simplified structure, such as the ANN with a single lag input and three hidden neurons in [19], and the ANN with two-lagged input and one hidden neuron in [20].

Meanwhile, a number of studies aim to develop novel models specifically for tourism demand forecasting, such as the logarithm least-squares support vector regression (LLS-SVR) in [21], Färe-Primont total factor productivity index in [22], neuro-fuzzy technique in [23], and optimal subset selection algorithm in [24].

In addition, in Appendix Table 7 and Appendix Table 8, we provide an overview of the use of traditional and machine learning models to make forecasting of tourism inflows in the last decade. The note underneath the tables explains the methodology abbreviations. To save the space of the main body in Appendix Table 7 and Appendix Table 8 is provided in the appendix of the paper.

Over the past twenty years, both the traditional and machine learning based tourism demand forecasting models have been thoroughly studied. The traditional models, although incorporating stochastic components as well as the macroeconomic variables and their covariance, are in the linear regression framework of either ARIMA or vector autoregressive (VAR). The assumptions behind those models fall into twofold: 1) the tourism demand time series contains a time-variant long-term trend, a seasonal trend, and a random error; 2) the two trends can be captured by linear model through either ARIMA or VAR framework. The idea of most ARIMA-family models assumes that the simple method such as differential removes the seasonality and the remained stationary time series can be modelled by the ARIMA structures with a seasonal component, i.e., SARIMA model. However, the stationarity feature has not been studied and proved, and a simple seasonal component cannot fully capture the time-variant strong seasonal patterns across time. The idea of the VAR-family models considers factors that impact the seasonal patterns and combines them as a vector for capturing their changes across time. The assumption of the VAR-family models is the linearity of those factors and that the covariance of the factors captures the seasonal changes. However, on one hand, the factors might not linearly impact the tourism demand. On the other hand, there are many factors that impact the tourism demand, and the factors might evolve across time. To model the factors effectively, a statistically principal structure, rather than a heuristic way, is required. On the other hand, the machine

learning based model has not been applied more than as just a basic black-box with an over-simplified structure, i.e., 1-2 lag input and one hidden neuron [19, 20]. Only a few studies have adequately customised the machine learning for the tourism application. However, those studies merely focus on the performance of data science model along without considering the domain-specific patterns.

A novel model, which considers the nature of the tourism data: a long term trend plus a strong time-variant seasonality, and takes the state-of-art machine learning model as a tailor-made framework specifically designed according to the data patterns, has yet to developed. Such a model shall consider the nonlinearity of the trend as well as the impacts of different economics and event factors by a statistical manner: regardless of the source of the impacts, their effects can be abstracted to a cyclical part, a jump part, an amplitude scale, and a stochastic error part. Considering all of those aspects, the model requires a complex tailor-made structure of certain machine learning models rather than a direct application.

This study seeks to make up for the above-mentioned research deficiency by putting forth a new model that adjusts computational techniques according to the data patterns. Despite being effective in capturing time series non-linearity, particularly in the case of detrend series [25], ANN may be less effective in representing strong seasonal patterns [25, 26]. Thus, this study draws upon earlier research [3, 6, 27, 28, 29] to develop a new hybrid model. Tourism data have been represented as a trend undergoing gradual alterations alongside a recurrent yearly peak and valley with somewhat dissimilar amplitudes. The proposed model is following the premise of the occurrence of the trend and seasonality, in keeping with [3, 6], while a mathematical tool is employed for explicit extraction of the two elements, conditional upon specific limitations of the seasonal elements, in keeping with [6, 27, 30]. Furthermore, the nonlinear approach applied by [6, 27] is adopted for ANN-based modelling of the trend element. Whilst to capture the seasonal patterns, a framework of hidden Markovian model outlined by [28, 29] is heavily extended with the multiplicative error model containing four components for the seasonally cyclical patterns, unexpected jump, event amplitude, and a random error term. In this way, the abilities of both ANN and hidden Markovian model are exploited to devise an application-specific technique to model equivalent aspects of tourism data. To the author's knowledge, no other study has proposed a technique involving the use of different computational models for modelling various data patterns.

The contribution of this work is mainly on the methodology part. First, this work introduces the multiplicative error model (MEM) structure into the tourism demand forecasting area. MEM has been commonly used in econometrics area in modelling financial volatility [29] and has been proved as a better choice in extracting the error term more cleanly, more consistent with large variability of the time series data and producing better forecasting performance [31] [32] [33]. Second, this work models the factors that impact the seasonal patterns with the idea of the hidden Markovian model, but through an extended format.

The seasonal component is modelled as a multiplicative format of three hidden Markovian states: a seasonal persistent cyclical component, a jump component capturing the positive or negative non-persistent (instantaneous) effect of certain events, and an amplitude component for event strength. Thus, regardless of the evolution of the factors, their impacts have been modelled via an abstracted format. Third, this work provides a novel framework of modelling the tourism demand: the trend and seasonality can be explicitly decomposed and captured separately with different models corresponding to their characteristics. The nonlinearity of the trend is modelled by the ANN and the unobservable factors that impact the seasonal patterns are modelled by the multiplicative Markovian chains.

The remainder of the study is organised in the following manner. Section 2 provides an in-depth presentation of the suggested model. Section 3 discusses the data and empirical research and assessment of the out-of-sample forecasting results. Section 4 provides the study conclusion.

2. Neural network enhanced hidden Markov STSM

We extend the Neural Network enhanced Structural Time Series Model (NNeSTSM) proposed in [6] by introducing the hidden Markovian process to model the seasonality component. We name the new model as Neural network enhanced hidden Markov Structural Time Series Model (NehM-STSM). In this model, we change the structure of the traditional STSM model in [14] and introduce the multiplicative error model (abbreviated as MEM), which was initially proposed in [34, 35], and further developed in [29]. We follow the MEM structure for two reasons:

1) The seasonality component of NNeSTSM in [6] is restricted to be a stationary autoregressive process with the mean value close to zero. The "valley" part of the seasonality component therefore contains negative values, which are not physically meaningful but merely show the decreasing period the data. As discussed in [29, 34, 35], the MEM guarantees the positivity of the modelled variables, which, otherwise, require additional transformation (i.e., log) or are ignored of the non-negativity. MEM structure has also been proved to perform well in time series data modelling by [33, 36]. By introducing MEM, our new model NehM-STSM generates non-negative seasonal components that keep the identical seasonality patterns as the original data and, on the other hand, shows a clear economic interpretation of the seasonal peak and valley.
2) Seasonality, which is observed from the data, is intrinsically driven by the population behaviours according to the weather, holiday, habit and other social causes, which may not be directly observable but its cyclical pattern has important impact on the forecasting accuracy [37]. Modelling the observed dynamics by its deep-rooted but unobservable causes allows the variable to switch abruptly between large number of states, which are generated by certain combinations of those causes and switch by a Markovian process. This methodology is usually called hidden Markov

model and is widely used in financial market [38], crime detection [28], and activity recognition as well [39]. Augustyniak et al show that a MEM framework can be easily incorporated with the unobservable states, which characterise the intrinsic nature and capture the style facts of the observed variables [29].

3) The primary impact factors of the seasonality include the weather, holidays, the habits, and the economic cycle and the unexpected events. Instead of incorporating them all into the model, a statistical principle is to extract and model the crucial patterns of impact factors. As the previous study [40], the factors affect the seasonality via three patterns: a persistence replicative component; a jump component capturing the unexpected event shock; a amplitude component for capturing the strength of the shock. MEM framework can be easily incorporated with the three patterns, which reflect the abstracted impact patterns.

Therefore, our model is established on the cornerstone of the traditional STSM in [14] while borrowing the advantage of the MEM format. Tourist arrival data is represented as the variable y_t. The NehM-STSM has a multiplicative error structure form [34] as

$$y_t = \mu_t \gamma_t, \tag{1}$$

where $t = 1, \dots, T$, μ_t and γ_t are trend and seasonal components respectively. We assume the process generating the seasonal component γ_t following the MEM form as

$$\gamma_t = V_t \omega_t, \tag{2}$$

where t=1, … , T, $\omega_t \sim D(1, \Phi_t^2)$ is a positive independent and identically distributed innovation process with mean 1, which is independent of V_t; and V_t is a process controlled by three hidden states: a seasonal persistence state driven by a high-dimensional Markov process; a jump state capturing the positive or negative shocking effect from certain non-persistent events from the market; and a data-driven state reflecting the amplitude of the event impact. The three hidden states represent the primary channels through which an impact factor may affect the seasonality. Regardless the source of the impact factors, their affection on the seasonality can be seen at either a replicative cycle or shocking effects with strong or weak strengths. The V_t is defined in detail in Section 2.3. As discussed before, the advantage of MEM is to maintain the positivity of the variable, i.e., seasonal component γ_t in equation (2). We follow the assumption in [14] that μ_t is a smooth and non-stationary process but leave its precise dynamics unspecified; and the seasonal component γ_t shows a recurrent cycle of peak and valley, which are controlled by unobserved states.

We implement the NehM-STSM in three steps. In the first step, we explicitly extract the trend component μ_t from the tourist arrival data y_t by the low-pass HP filter subject to the stationary constraint of the seasonal component, which can subsequently be obtained as $\gamma_t = y_t/\mu_t$. In the second step, we apply the

AutoRegressive Neural Network (ARNN) on μ_t. The *n*-step value of y_{t+n} can therefore be forecasted via the trained ARNN. In the third step, the seasonal component γ_t is modelled by the hidden states defined in equation (2). The *n*-step ahead value of γ_{t+n} is obtained via the estimated model. This procedure allows us to forecast the *n*-step ahead future value of the tourist arrival y_{t+n} by $y_{t+n} = \mu_{t+n}\gamma_{t+n}$. The three steps are discussed in detail below.

2.1 The 1st Step: decomposing the trend and seasonality

The low-pass Hodrick-Prescott filter (HP filter) developed by [41] is adopted for extraction of the trend element μ_t in keeping with the methodology proposed by [6]. In the field of macroeconomics, the HP filter is a popular tool for extraction of the short-run cyclical element and discovery of a time series trend [42, 43, 44]. The μ_t can be determined in the NehM-STSM by calculating the following formula using certain values of smoothing parameter λ:

$$\min_{\mu_t}\left(\sum_{t=1}^{T}(y_t - \mu_t)^2 + \lambda \sum_{t=2}^{T-1}[(\mu_{t+1} - \mu_t) - (\mu_t - \mu_{t-1})]^2\right) \quad (3)$$

In the above, the fluctuation in the μ_t growth rate is penalised by λ, the penalty being greater and μ_t being smoother, the larger λ is. The λ value is calculated by using the statistical criteria, the Augmented Dickey-Fuller (ADF) test [45], in accordance with the approach applied by [6]. The null hypothesis associated with the ADF specifies that the seasonal element γ_t contains a unit root and if this hypothesis is invalidated, then γ_t is stationary. For selection of a suitable λ value, the empirical value suggested by [46, 47], namely, λ = 129600, is used as a starting point, proceeding down to zero. The μ_t is extracted for every λ value and γ_t stationarity is computed and assessed until invalidation of the hypothesis.

The selection of λ is exemplified in Figure 1 based on monthly data of inflow of UK tourists to the US during January 1996-September 2017. In Figure 1(a), the λ is determined to be 129600 (1600×3^4) for data per month, in keeping with the empirical research conducted by [46, 47]. Meanwhile, in Figure 1(b)-(d), there is a reduction in λ value to 3600, 1600 and 210, respectively. The emerging pattern reveals that the decrease in λ reduces the smoothness of the trend element, while the resulting seasonality element gradually becomes a stationary seasonal process. The λ value of 210 generated by the selection process is associated with a *p*-value of high significance (0.001) for the ADF test (Figure 1d). Meanwhile, intermediate λ values related to the selection process are indicated in Figure 1(b) and Figure 1(c).

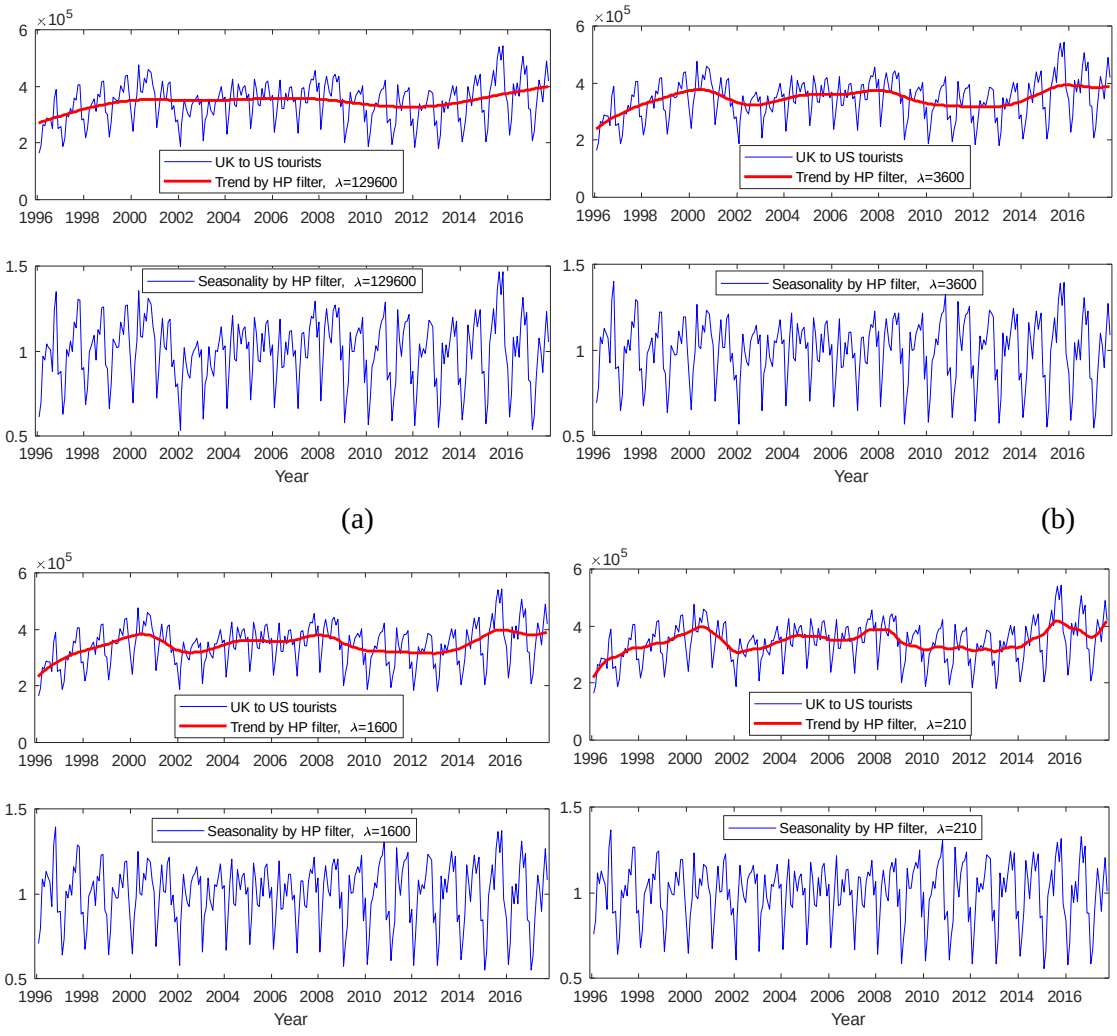

Figure 1 Use of HP filter to break down the trend and seasonality with various $\boldsymbol{\lambda}$ values. The superior portions of (a)-(d) show the blue curves denoting the monthly inflow of UK tourists to the US during January 1996-September 2017 and the red curves denoting the trend element by HP filter with $\boldsymbol{\lambda}$ having a value of 129600, 3600, 1600 and 210, respectively. The lower portions of (a)-(d) show the blue curves denoting the equivalent seasonal element derived as the ratio of the arrival data and the trend element, respectively

2.2 The 2nd Step: Trend element modelling

Once the trend and seasonal elements are broken down, μ_t is subjected to an Auto-regressive Neural Network (ARNN), which is a popular tool for modelling time series and has been demonstrated to have a better performance not only compared to conventional models in the deseasonalised financial literatures [25, 26, 48, 48], but also compared to repetitive feed-forward neural network [49]. Furthermore, as reported by [6], ARNN is especially effective in capturing the non-linearity of deseasonalised data related to tourism inflows. In the case of one-step-ahead forecasting, ARNN takes the form outlined by [49, 50]:

$$\hat{L}_t(\theta_{\mathrm{ARXNN}}) = g[\varphi_i(t), \theta_{\mathrm{ARNN}}] = F_j \sum_{u=1}^{N_h} W_{j,u} f_u\left(\sum_{i=1}^{N_u} \varphi_i(t) w_{u,i} + w_u\right) + W_j \quad (4)$$

where, the ARNN function is denoted by $g[\varphi_i(t), \theta_{\mathrm{ARNN}}]$, the number of neurons at the hidden layer and the number of input variables are respectively denoted by N_h and N_u, the weights factor from the neurons

at the hidden layer to the neurons at the output layer is denoted by $W_{j,u}$, the matrix containing the weights from the neurons at the input layer N_u to the neurons at the hidden layer is denoted by $w_{u,i}$, the biases of hidden and output layers are respectively denoted by w_u and W_j, while the vector containing the regressive coefficients of the neural network AR part and the parameters vector containing every modifiable neural network parameter are respectively denoted by $\varphi_i(t)$ and θ_{ARXNN}. In keeping with several studies [6, 49, 50], the ARNN configuration employed in this study is N_u=4, and N_h=10, signifying that the input layer comprises four neurons equivalent to the 4-lag inputs, the hidden layer consists of ten neurons, each of which contains a hyperbolic tangential activation function, and the output layer comprises a single neuron equipped with linear regression function. Hence, the existing value of μ_t and the preceding three lags (μ_{t-1}, μ_{t-2}, and μ_{t-3}) are the basis for forecasting. As a supervised-learning neural network, it involves "training" of the model parameters for mapping the input-output variables based on the adjusted Levenberg-Marquardt algorithm [51], which is intended to reduce the maximum gradient to attenuate the quadratic error.

Based on the same data as in Figure 1, Figure 2 exemplifies forecasting of the trend element, the extraction of which is undertaken with HP filter with an λ value of 210 based on trained ARNN. The training of the ARNN model is achieved with the trend element data covering the period January 1996-July 2013, while ARNN out-of-sample testing is performed on the basis of the rest of the data from the period August 2013-September 2017. The predicted (red colour) and extracted trend elements can be seen in the superior portion of Figure 2, exhibiting an extremely closed pattern. Meanwhile, the absolute error of the predicted trend is indicated in the middle portion and the absolute percentage error of the predicted trend is shown in the inferior portion of Figure 2. It can be seen that performances display an extremely high level of competitiveness, with less than 0.6% error.

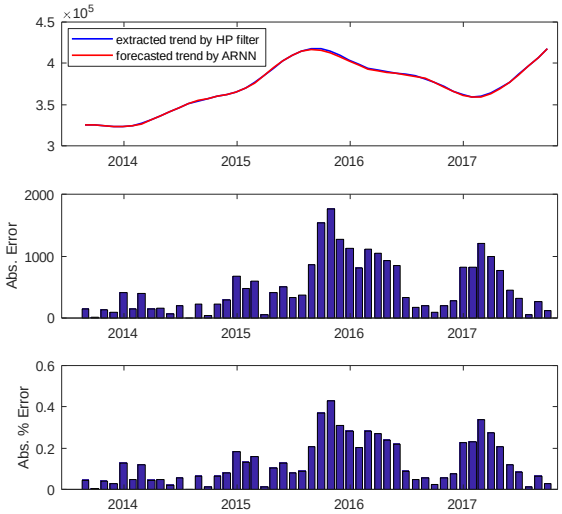

Figure 2 Application of the ARNN model for forecasting of the trend element. The upper graph shows the extraction of the trend element (blue curve) from the monthly data of inflow of UK tourists to the US during August 2013-September 2017 based on the

HP filter with $\boldsymbol{\lambda = 200}$. The red curve denotes the trend predicted by ARNN, the training of which was undertaken based on trend element data from January 1996-July 2013. The middle graph indicates the absolute error of the predicted trend, while the lower graph shows the absolute percentage error of the predicted trend.

2.3 The 3rd Step: Seasonal element modelling

In the third step, we estimate a process by equation (2) for the seasonal component $\gamma_t = y_t/\mu_t$ as

$$\gamma_t = V_t \omega_t, \tag{5}$$

where t=1, … , T, $\omega_t \sim D(1, \Phi_t^2)$ is a positive independent and identically distributed innovation process with mean 1, which is independent of V_t. Following the two regime Markovian-switching model of [52], and the structure of multiplicative time series model of [29, 33], we model the process V_t as a multiplicative format of three hidden Markovian states as

$$V_t = S_t J_t L_t, \tag{6}$$

where S_t represents the seasonal persistent component by a multiplication of N Markovian processes; J_t is a jump state capturing the positive or negative non-persistent (instantaneous) effect of certain market or social events, i.e., the positive events such as musical festival, Oktoberfest, Olympic games and FIFA world cup and the negative events such as natural disaster, infectious disease and terrorism attack; and L_t is the event impact amplitude based on historical data.

The construction of S_t

S_t is defined by a multiplicative format of N Markovian processes, which are illustrated by $S_t^{(i)}$, i=1, … , N, as

$$S_t = S_0 \prod_{i=1}^{N} S_t^{(i)}, \tag{7}$$

where $S_0 = \frac{1}{E\left[\prod_{i=1}^{N} S_t^{(i)}\right]}$ is a scaling parameter that makes the mean of S_t to be 1: $\mathrm{E}[\mathrm{S_t}]$=1. Each of the N Markovian processes has two states and shares the same transition matrix as

$$P = \begin{bmatrix} p & 1-p \\ 1-p & p \end{bmatrix} \tag{8}$$

where $p \in (0,1)$. Each Markovian process has distinct state as $S_t^{(i)} \in \{s_i, 1\}$, where $s_1 > 1$ and

$$\begin{aligned} s_i &= (1-\theta_s) + \theta_s s_{i-1} \\ &= 1 + \theta_s^{i-1}(s_1 - 1) \end{aligned}$$

where i=2, … , N and $\theta_s \in [0,1]$. The scaling parameter can be calculated as

$$S_0 = \frac{1}{E\left[\prod_{i=1}^{N}\left(1 + \theta_s^{i-1}(s_1 - 1)\right)\right]}.$$

Based on this, we can have $s_1 \geq s_2 \geq \cdots \geq s_N \geq 1$. In each Markovian process, at time t, if the component $S_t^{(i)} = 1$, it does not contribute to the variation of the seasonal component γ_t; and if the component $S_t^{(i)} = s_i$, it pushes up or pulls down the variation of the γ_t. We therefore define $S_t^{(i)} = 1$ and $S_t^{(i)} = s_i$ as the "off" and "on" state respectively. It is noted that at the "on" state, $S_t^{(N)}$ and $S_t^{(1)}$ have the weakest and strongest effect on the seasonality component respectively. The component $S_t^{(i)}$ satisfies the intuition and assumption of the model structure: the s_i is determined by state values of $S_t^{(i)}$ in "last season" with different impacts, which is represented by "on" with value s_i or "off" with value 1. For example, following the assumption of 12 "seasons" in a year in [6], we have N=12 in equation (7). Therefore, each value of S_t in the current year is a combined effect of seasonal patterns $S_t^{(i)}$, i=1, … , N in last year with each of the patterns $S_t^{(i)}$ being an independent Markovian process. If one of the processes is switched "on", the seasonal pattern in this year increases or decreases proportionally to the magnitude of the pattern in last year, measured by the value of s_i. The seasonal effect remains for several periods following the geometric distribution with the transition probability of p. S_t, the result of the final state is produced by the multiplicative combination of the N Markovian independently evolved processes.

Moreover, if we take the log-transformation to two sides of equation (7), we can have

$$\log S_t = \log S_0 + \sum_{i=1}^{N} \log S_t^{(i)}, \tag{9}$$

As the study in [53], the Markovian process with two states can be illustrated as an autoregressive of order 1, AR(1), process. Furthermore, [54] argued that a model with structure of a sum of AR(1) processes can capture the long term dependence of the log-transformed financial data. Consequently, in this study, the log-transformed seasonal persistent component S_t can be represented as the sum of N AR(1) processes, each of which is interpreted as the corresponding process in last "season". Thus, seasonal persistent component S_t in our proposed NehM-STSM model can be considered as a discrete version of the model in [54] applied in tourism area.

The construction of J_t

Similarly, the process J_t is defined by a sequence of independent and identical distributed random variables with discrete probability density function (also termed as probability mass function) as

$$P(J_t = j_0 \times j_i) = \begin{cases} q(N-1)^{-1}, i = 1, \dots, N-1, \\ 1-q, \qquad i = N, \end{cases} \tag{10}$$

where $q \in (0,1), j_1 > 1$, therefore we can have

$$\begin{aligned} j_i &= \left(1 - \theta_j\right) + \theta_j j_{i-1} \\ &= 1 + \theta_j^{i-1}(j_1 - 1) \end{aligned}$$

where i=2, … , N, $\theta_s \in [0,1]$, $j_N = 1$ and therefore $j_1 \geq j_2 \geq \cdots \geq j_N = 1$. The scaling parameter j_0 can be calculated as $j_0 = \left[1 + q\,\frac{(j_1-1)\left(1-\theta_j^{N-1}\right)}{(N-1)\left(1-\theta_j\right)}\right]^{-1}$ to maintaining $E[J_t] = 1$. The J_t is interpreted as a jump state that captures the positive or negative instantaneous impact of certain market or social events on the seasonality. The parameter q is the probability of the event occurring in a given time period. In practice, the events occurring simultaneously has a cumulative effect on the certain variable. In our model, the cumulation is interpreted by the multiplicative structure, which is given by one of the values $j_1, j_2, \ldots, j_{N-1}$ with the equal probability q. The j_1 represents the strongest impact and the j_{N-1} has the weakest effect. The probability of no event is $1 - q$. In contrast to S_t, the effect of certain event generated by J_t does not last for long time and therefore generates instantaneous jumps of different magnitudes on the seasonality component V_t. Since we assume N=12 in equation (7), we also have N=12 for J_t component. But for the value of J_t at time t, we only assume one event occurring, either any of j_i, i=2, … , $N - 1$, or $i = N$, which is associated with $j_N = 1$ (off state).

The construction of L_t

L_t is defined as a novel component to capture the time-varying effect of the event. The intuition of L_t is to capture the season-on-season changes of the component V_t. L_t is defined as

$$L_t = \prod_{i=1}^{N_L} L_t^{(i)}, \tag{11}$$

$$L_t^{(i)} = 1 + l_i \frac{r_{t-i}}{\sqrt{L_{t-i}}}, \tag{12}$$

where $i = 1,\ldots, N_L$, $l_1 > 0$, $l_i = \theta_l^{i-1} l_1$ for $i = 2,\ldots, N_L$, $\theta_l \in [0,1]$, and N is the number of the seasons in a year. As the construction of S_t assumes 12 "seasons" in a year, the value of N in equation (11) is also configured as N=12. The assumption of L_t is that the amplitude value at time t is determined by the season-on-season "return" r_{t-N-i} up to time t-1. For example, as we assume 12 "seasons" in a year by using monthly tourism data, the season-on-season "return" at June 2017 $r_{June,2017}$ is defined as the return of seasonal component $V_{June,2017}$ at June 2017 to that of June 2016 $V_{June,2016}$ as

$$r_{June,2017} = \frac{V_{June,2017} - V_{June,2016}}{V_{June,2016}}.$$

Consequently, the component L_t at July 2017 is determined by the last N_L season-on-season "returns". In this study, we assume an event having the impact on the seasonality for half year at the most, thus having N_L=6. When the "return" is positive, $r_{t-i} > 0$, the component $L_t^{(i)}$ is higher than 1 therefore enhancing the impact on the seasonality. On the other hand, when the "return" is negative, $r_{t-i} < 0$, the component $L_t^{(i)}$ is lower than 1 therefore lowering the seasonal component V_t. Based on this structure, the impact of the events

on the seasonal component is influenced by the importance of the event, which is measured by the magnitude of the return r_{t-i} and of a multiplicative factor l_i giving less weights to more distant events.

The model structure of seasonal component γ_t

As the discussion, the seasonal component γ_t has the structure of multiplicative Markovian processes, each of which evolves independently. Figure 3 shows an example of the multiplicative Markovian processes. $V_{t-1}^{(1)}$, $V_{t-1}^{(2)}$, …, and $V_{t-1}^{(N)}$ are N independent two-state Markovian processes. The final state is combined as a product of the N processes.

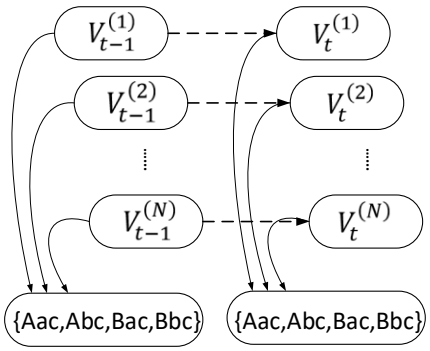

Figure 3 This figure shows an example of the structure of multiplicative hidden Markovian processes. In this example, the Markovian state $\boldsymbol{V_{t-1}^{(1)}} \in \{\boldsymbol{A}, \boldsymbol{B}\}$, $\boldsymbol{V_{t-1}^{(2)}} \in \{\boldsymbol{a}, \boldsymbol{b}\}$, and $\boldsymbol{V_{t-1}^{(N)}} \in \{\boldsymbol{C}, \boldsymbol{c}\}$. The final state is the product of $\boldsymbol{N}$ processes.

The economic interpretation of the two-state Markovian model was indicated in [52] as a mimic of a "volatile versus tranquil" two-period market, i.e., bull versus bear period. However, real market typically contains much higher number of states than the two-state model. Therefore, a multiplicative structure offers a more realistic way on this issue. Let us consider the seasonal persistent component S_t modelled by N hidden Markovian states, which can be expressed as:

$$S_t\left(S_t^{(1)}, S_t^{(2)}, \dots, S_t^{(N)}\right) = \delta\left(S_t^{(1)}\right)^T \begin{vmatrix} 1 \cdot \left(S_t^{(2)}, \dots, S_t^{(N)}\right) \\ s_1 \cdot \left(S_t^{(2)}, \dots, S_t^{(N)}\right) \end{vmatrix},$$

$$1 \cdot \left(S_t^{(2)}, \dots, S_t^{(N)}\right) = \delta\left(S_t^{(2)}\right)^T \begin{vmatrix} 1 \cdot 1 \cdot \left(S_t^{(3)}, \dots, S_t^{(N)}\right) \\ 1 \cdot s_2 \cdot \left(S_t^{(3)}, \dots, S_t^{(N)}\right) \end{vmatrix},$$

$$s_1 \cdot \left(S_t^{(2)}, \dots, S_t^{(N)}\right) = \delta\left(S_t^{(2)}\right)^T \begin{vmatrix} s_1 \cdot 1 \cdot \left(S_t^{(3)}, \dots, S_t^{(N)}\right) \\ s_1 \cdot s_2 \cdot \left(S_t^{(3)}, \dots, S_t^{(N)}\right) \end{vmatrix},$$

… …,

where $S_t^{(i)} \in \{1, s_i\}$ is the state variable in the #i Markovian process ($i = 1, \dots, N$), and $\delta\left(S_t^{(i)}\right)^T$ is a 2-dimensional vector with unity value at $S_t^{(i)}$ and zero at others. The seasonal component S_t is therefore

constructed with N layers. The 1st layer, $i = 1$, determines whether the value of the seasonality is at the peak level. The second layer breaks each of the two states at the 1st layer into further two states to increase the granularity. For example, $s_1 \cdot s_2 \cdot \left(S_t^{(3)}, \dots, S_t^{(N)}\right)$ means that the seasonality lies in the "higher" state (s_2) of the "peak" level (s_1), i.e., $s_1 = 1.99$ and $s_2 = 1.50$ in our empirical studies. The interpretation of more layers is analogous. In our case of 12 seasons in a year, N=12, the model partitions the seasonality to 12 layers (through the hidden states), each of which may be switched "on" or "off" to determine the value of the current seasonality at time t.

Estimating the Seasonal Component V_t

Seasonal component V_t is constructed as a multiplicative format of three hidden Markovian states $V_t = S_t J_t L_t$ with $N \times 2^N$ elements state-space $\boldsymbol{X}_V$. The model can be estimated using the standard Hamilton filter [52] with N=12. The conditional density of the observed process can be calculated as:

$$p(\gamma_t|F_{t-1}, \Theta) = \sum_{V_t \in \boldsymbol{X}_V} p(\gamma_t|V_t, F_{t-1}, \Theta) p(V_t|F_{t-1}, |\Theta),$$

the filtering distributions of the hidden states can be obtained as:

$$p(V_t|F_t, \Theta) = \frac{p(\gamma_t|V_t, F_{t-1}, \Theta) p(V_t|F_{t-1}, \Theta)}{p(\gamma_t|F_{t-1}, \Theta)},$$

and predictive distributions of the hidden states can be obtained as

$$p(V_t|F_{t-1}, \Theta) = \sum_{V_t \in \boldsymbol{X}_V} p(V_t|V_{t-1}, F_{t-1}, \Theta) p(V_{t-1}|F_{t-1}, \Theta),$$

where γ_t is the observed seasonal component in equation (1), Θ represents the model parameters as $\Theta = \{p, \theta_s, s_1, q, \theta_j, j_1, \theta_l, l_1\}$. The log-likelihood estimation function is then obtained as

$$\log p(\gamma_1, \dots, \gamma_T|\Theta) = \sum_{t=1}^{T} \log p(\gamma_t|F_{t-1}, \Theta).$$

For the initialization of the Hamilton filter, the state distribution at time t=1, $p(V_t|F_0, \Theta)$ has been made as the stationary distribution of the Markovian chain. The code of estimating this multi-dimensional hidden Markovian model is available as the supplementary material.

By those three steps discussed in Section 2.1-2.3, our Neural network enhanced hidden Markov Structural Time Series Model (NehM-STSM) is implemented and estimated. The estimation of the trend μ_t and seasonal γ_t components are completely separated. Because of this, the *n*-step ahead forecast of the monthly tourist arrivals is also separated by the ARNN in Section 2.1 and multiple hidden Markovian model in Section 2.3. The final forecasting output is the multiplication of the results from two models according to the deterministic equation (1): $\hat{y}_{t+n} = \hat{\mu}_{t+n} \times \hat{\gamma}_{t+n}$.

3. Assessment of forecasting

3.1 Model and Data

The three models chosen for assessment and comparative analysis of their forecasting performance are the suggested Neural Network-enhanced hidden Markov Structural Time Series Model (NehM-STSM), the Neural Network-enhanced Structural Time Series Model with HP filter (NNeSTSM-HP), and the Neural Network-enhanced Structural Time Series Model with Moving Average as the trend filter (NNeSTSM-MA). [6] were the ones who put forth the second two models, which performed better compared to the conventional Seasonal Autoregressive Integrated Moving Average model (SARIMA). The structural similarity of these two models to the NehM-STSM is the reason for selecting them as reference models in the present study.

The suggested model is analysed empirically by drawing on monthly data of inflows of tourists from twelve major source markets (i.e. Mexico, Canada, Mainland China, Japan, UK, South Korea, Brazil, Germany, Australia, France, Italy, Spain) to the US in the period between January 1996 and September 2017. The official website of the *National Travel & Tourism Office* was the source of the time series data for every source market. Figure 4 provides the data series of the tourism inflow from the twelve major source markets during January 1996-September 2017. It can be seen that there has been a significant rise in the inflow of tourists from Mexico and Mainland China between 2010 and 2016. It is also worth observing that the inflow of tourists from all source markets into the US exhibits a significantly seasonal pattern.

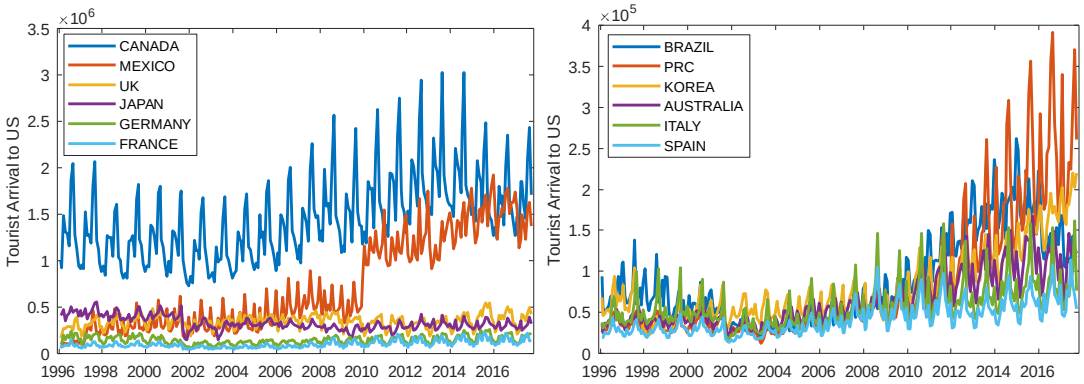

Figure 4 Data of tourism inflow to the US during January 1996-September 2017; (a) inflow of tourists from the first six source markets (i.e. Canada, Mexico, UK, Japan, Germany, France); (b) inflow of tourists from the following six source markets (i.e. Brazil, Mainland China, South Korea, Australia, Italy, Spain)

A rolling-window forecasting mechanism is used to assess the forecasting performance. More specifically, model estimation is based on the rolling-window data, while testing is based on the rest of the following-up data. The period January 1996-December 2009, the first 70% of the whole dataset, represents the original

window *W1*, while the rest of the data from the period January 2010-September 2017 serve as the testing dataset. Initially, the data in *W1* is used for training the models, while afterwards the testing dataset from the period January 2010 to June 2011 is used for evaluating the models for a set of horizon *h* of one to eighteen months ahead forecasting. Subsequently, the original window for model estimation moves one month ahead to *W2* spanning the period February 1996-January 2010, while model testing is based on the rest of the data for the period February 2010 to July 2011, with a set of horizon *h* of one to eighteen months ahead forecasting. Likewise, model estimation and forecasting are performed recurrently up to the point where no more remainder data are available. In the last round, the model is trained by the data in the period of April 2003 to March 2016 and tested by the data in the period of April 2016 to September 2017, a set of horizon *h* of one to eighteen months ahead forecasting. Eventually, the rolling-window forecasting mechanism yields 88 sets (one-month sliding from January 1996 to April 2003) of *h* (*h*=1, …, 18) months-ahead forecasting amounting to 88*18*12= 19008, with 1584 forecasting in every one of the twelve source markets.

The widely used Mean Average Absolute Percentage Error (MAPE), calculated as MAPE=$\frac{|\hat{y}-y|}{y} * 100\%$, where $\hat{y}$ is the forecasted result, is chosen as the measure of forecasting precision in order to encompass all results. An additional common measure employed for assessment of all results is the Root Mean Square Error (RMSE), calculated as RMSE=$\sqrt{\frac{\sum_{i=1}^{N}(\hat{y}-y)^2}{N}}$, where $\hat{y}$ is the forecasted result and the *N* is the total number of forecasting results (see Appendix). Furthermore, the predicted values of tourism inflow are represented as a closer insight example.

3.2 Empirical Result

The average MAPE and RMSE error measures associated with the twelve tourist inflow series for every forecasting horizon are illustrated in Figure 5. It is apparent that the lowest performance is exhibited by the NNeSTSM-MA model, while NNeSTSM-HP and NehM-STSM have a similar performance. Furthermore, the error rate of NehM-STSM is somewhat lower from horizon 1-15. However, NehM-STSM has a markedly greater performance than NNeSTSM-HP when the forecasting horizon exceeds 15.

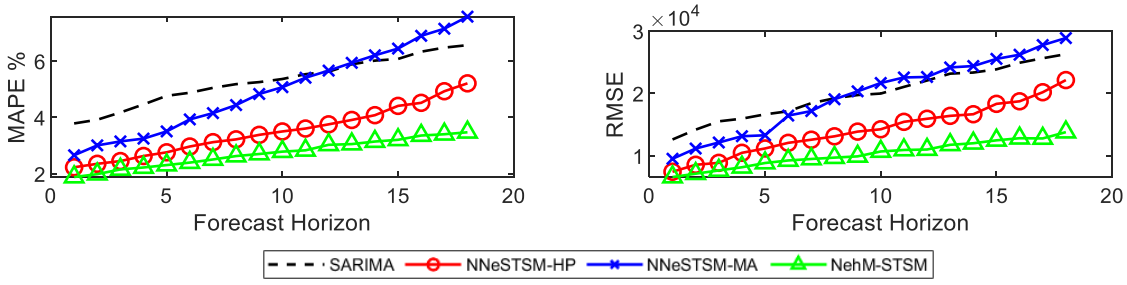

(a) (b)

Figure 5 The **MAPE** and **RMSE** for different horizon, with an average of these two measures being generated across all twelve markets. Figure 7 provides the MAP of every market. NehM-STSM = Neural Network-enhanced hidden Markov Structural Time Series Model; NNeSTSM-HP = Neural Network-enhanced STSM model with HP filter; NNeSTSM-MA = Neural Network-enhanced STSM model with Moving Average as the trend filter; SARIMA = Seasonal autoregressive integrated moving average.

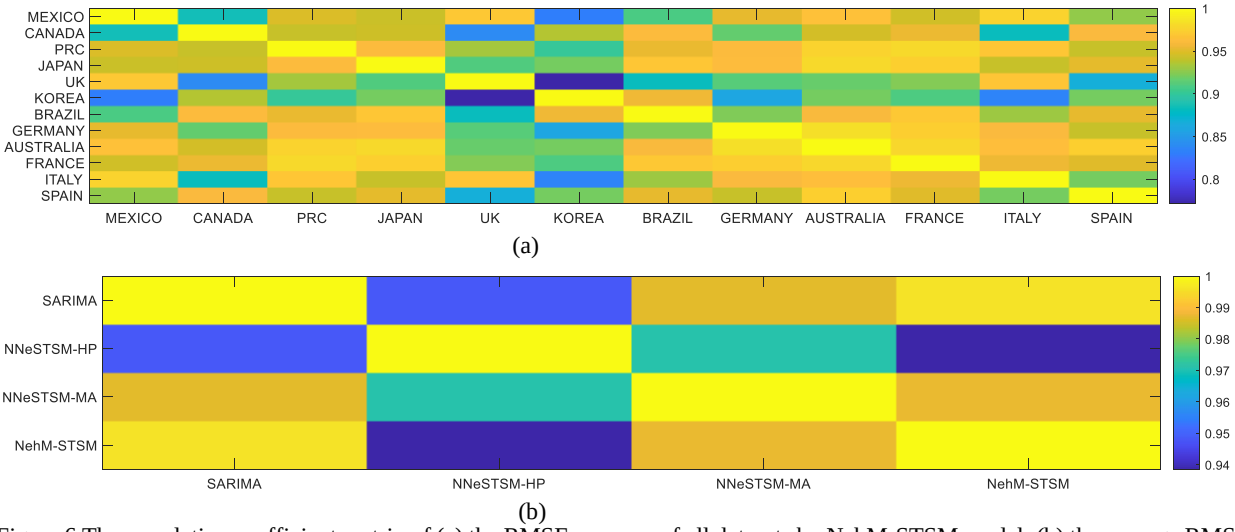

(a)

(b)

Figure 6 The correlation coefficient matrix of (a) the RMSE measure of all datasets by NehM-STSM model; (b) the average RMSE measure across all twelve markets by four different models SARIMA, NehM-STSM, NNeSTSM-HP, and NNeSTSM-MA.

An in-depth perspective of forecasting precision is outlined in Figure 7, which shows the MAPE and RMSE measures for forecasting outcomes of horizon h=1 to 18 (1 month to 1.5 years) with data from twelve source markets (Japan, Mainland China, Canada, Mexico, France, UK, Korea, Italy, Australia, Germany, Spain, Brazil). From the forecasting horizon 1 to 5 months ahead, the two models, NehM-STSM and NNeSTSM-HP perform similarly, although NehM-STSM, indicated by the green line, has a slightly higher performance than the other two in the majority of cases. The model NNeSTSM-MA, however, does not provide a stable forecasting performance across twelve datasets. On the datasets of P.R.C, Canada, UK, Australia, Italy, and Spain, the NNeSTSM-MA performs close to NNeSTSM-HP in the forecasting horizon 1 to 5 months ahead. But on other datasets, the NNeSTSM-MA apparently shows higher error than NNeSTSM-HP and NehM-STSM models. The SARIMA, however, performs the worst overall except the cases of Mexico, UK, and Australia data, where the SARIMA beats the NNeSTSM-MA model in long horizon forecasting. This is

usually due to the structural change in the tourism demand data in the long term and thus the moving average being unable to capture the long-term trend.

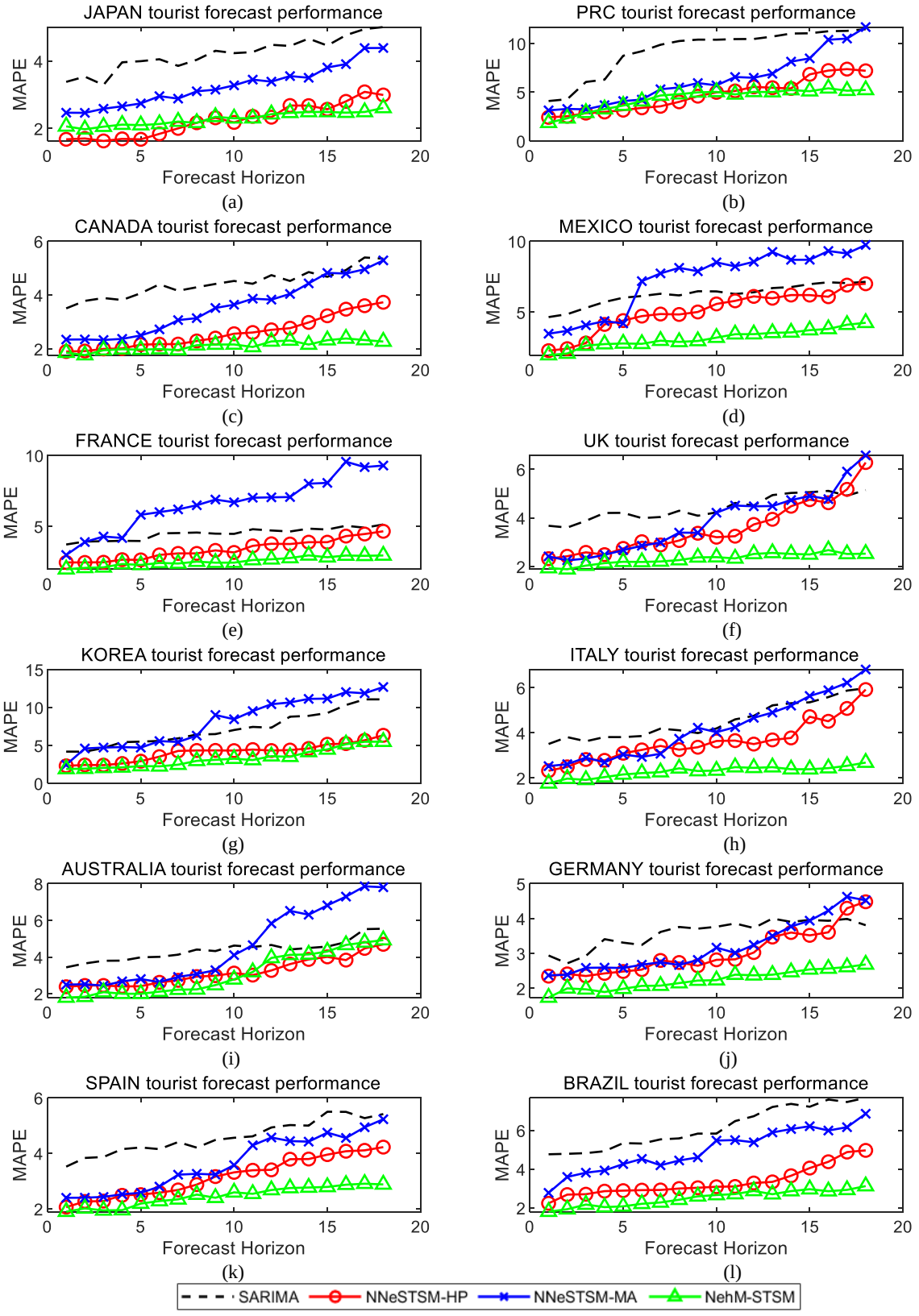

Figure 7 Forecasting error measures of MAPE achieved by the SARIMA, NNeSTSM-HP, NNeSTSM-MA and NehM-STSM models regarding tourist inflows from twelve source markets (Japan, Mainland China, Canada, Mexico, France, UK, Korea, Italy,

Australia, Germany, Spain, and Brazil). Model estimation is based on data from the period January 1996-December 2009, which are summarised in the graphs to ensure clarity. The forecasting outcomes cover the period January 2010-September 2017. NehM-STSM = Neural Network-enhanced hidden Markov Structural Time Series Model; NNeSTSM-HP = Neural Network-enhanced STSM model with HP filter; NNeSTSM-MA = Neural Network-enhanced STSM model with Moving Average as the trend filter.

The seasonality component is the sole point of dissimilarity between NehM-STSM and NNeSTSM-HP, since they both involve application of the HP filter and ARNN. The existence of a correlation between the value of the seasonal element at time *t* and the values of seasons in the previous year via different formats is the assumption underpinning both models. Furthermore, the premise adopted by NehM-STSM is that the noted variables are produced by latent states through the assembly of a multiplicative structure of twelve hidden Markovian processes for capturing seasonal patterns. Meanwhile, the premise adopted by NNeSTSM-HP is that the seasonal element is associated with a conventional additive structural STSM model. Seasonal element modelling with these two models is exemplified in Figure 8. The seasonal element of tourist inflow from Mexico is predicted by STSM (Figure 8a) and hidden Markovian processes (Figure 8b). Regarding the absolute percentage error (APE), hidden Markovian processes have a significantly lower forecasting error compared to STSM. The results obtained for the seasonal element of the tourist inflow from Canada do not differ much (Figure 8c and d). Dictating the seasonality at time *t* by turning the twelve layers (states) "on" or "off", the multiple layer (state) structure of the multiplicative hidden Markovian processes model is the reason for the reduced error rate associated with this model.

The seasonal element is defined as $\gamma_t = y_t/\mu_t$, by the multiplicative structure of equation (1), meaning that γ_t is a cyclical variable with a mean of 1. On the other hand, in NNeSTSM-HP, the seasonal element has a mean of zero but with high deviation because it is defined as the discrepancy between y_t and μ_t, which are the original tourist arrival and the trend element, respectively. The stability and economic relevance of the seasonal element are improved by the multiplicative definition of the NehM-STSM, with γ_t values of 0.8 and 1.2 respectively suggesting that tourist arrival is around 80% of the dominant trend and exceeding the trend by 20%.

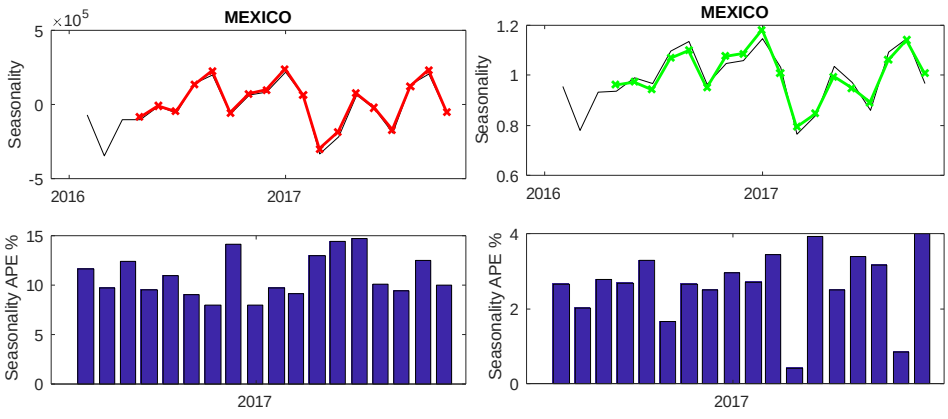

(a) (b)

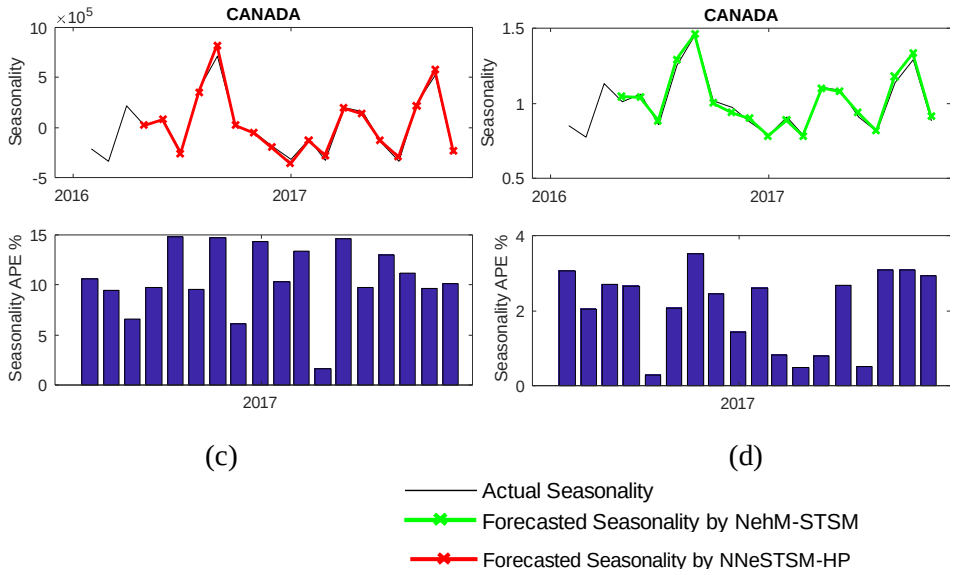

Figure 8 The forecasted seasonal element of tourist inflow and APE (%). The outcomes of Mexican tourist inflow are presented in (a) and (b), while the outcomes of Canadian tourist inflow are presented in (c) and (d). NehM-STSM = Neural Network-enhanced hidden Markov Structural Time Series Model; NNeSTSM-HP = Neural Network-enhanced STSM model with HP filter; NNeSTSM-MA = Neural Network-enhanced STSM model with Moving Average as the trend filter. The forecasting is based on the 1-month ahead rolling-window mechanism.

For instance, the approximated parameter

$$\{p, \theta_s, s_1, q, \theta_j, j_1, \theta_l, l_1\}$$

is reported for the seasonality element $V_t = S_t J_t L_t$ of the NehM-STSM model applied to Mexican tourist inflow to the US. Based on the data of Mexican tourist inflow to the US, the approximated parameters for the seasonal element V_t of NehM-STSM are listed in Table 1. The parameter suggests that the likelihood of the element S_t hidden state switching "on" is nearly 1 (p = 0.9788), while the likelihood of events altering seasonality is more or less small (q = 0.1388).

Table 1 The seasonality element $\boldsymbol{V_t}$ of the NehM-STSM model based on data of Mexican tourist inflow to the US

	Tourist arrival from Mexico
Markovian component:	$p = 0.9788, \theta_s = 0.82, s_1 = 2.18$ $s_1 = 2.18, s_2 = 1.52, s_3 = 1.27, s_4 = 1.15, s_5 = 1.08, s_6 = 1.04,$ $s_7 = 1.03, s_8 = 1.02, s_9 = 1.01, s_{10} = 1.00, s_{11} = 1.00, s_{12} = 1.00$
Event component:	$q = 0.1388, \theta_j = 0.76, j_1 = 3.55$ $j_1 j_0 = 3.09, j_2 j_0 = 2.53, j_3 j_0 = 2.13, j_4 j_0 = 1.82, j_5 j_0 = 1.61, j_6 j_0 = 1.42,$ $j_7 j_0 = 1.29, j_8 j_0 = 1.20, j_9 j_0 = 1.16, j_{10} j_0 = 1.11, j_{11} j_0 = 0.89, j_{12} j_0 = 0.46,$
Event amplitude component:	$\theta_l = 0.91, l_1 = 0.45$

The original outcomes in Figure 7 are supplemented in Table 2 to Table 7 with error measures of the predicted monthly tourist inflows for every horizon from six source markets. NehM-STSM exhibits a markedly and consistently higher performance than the NNeSTSM models in all cases, apart from the points underscored in Table 2 and Table 3. As highlighted by [6], the series associated with Japan and Mainland China exhibit patterns that are significantly different. The inflow of Japanese tourists generally exhibits

stability, aside from a notable decline in 2001 owing to the 9/11 terrorist attack. Meanwhile, during 2010-2017, the inflow of Japanese tourists exhibits repeated patterns that are more or less similar. On the other hand, there is an approximately 800% rise in the inflow of tourists from Mainland China, from 0.5×10^5 in 1996 to 4×10^5 in 2017. The trend and seasonal elements both exhibit stability during the period 1996-2008. By contrast, in the period post-2008, there is a rapid rise in the trend element, whereas the seasonal element displays yearly fluctuation with discrepant magnitude. These kinds of patterns make the hidden states inaccurate because they are not intended for structural break change. Regarding the inflow of Chinese tourists to the US, the "opening up policy" implemented by the Chinese government is a notable contributing factor to the observed figures, particularly after 2008, when Beijing played host to the Olympic Games.

Table 2 The average precision of monthly forecasting of inflow of Japanese tourists to the US. MAPE and RMSE are averaged across all predicted data during the period August 2013-September 2017, while model estimation is based on the data from the period January 1996-July 2013.

JAPAN	MAPE (%)			RMSE		
Horizon	NNeSTSM-HP	NNeSTSM-MA	NehM-STSM	NNeSTSM-HP	NNeSTSM-MA	NehM-STSM
1	**1.4181**	2.0708	**1.7549**	**4,054.2216**	5,947.8787	**4591.2257**
2	**1.4251**	2.1153	**1.7746**	**4,116.4230**	6,020.8353	**4908.9931**
3	**1.4387**	2.2448	**1.7970**	**4,940.8339**	6,933.7099	**4926.8026**
4	**1.4761**	2.2996	**1.8316**	**4,970.5450**	7,182.1324	**5107.0065**
5	**1.4971**	2.4668	**1.8736**	**4,999.1695**	7,203.4253	**5314.2614**
6	**1.6709**	2.5655	**1.9252**	**5,221.7649**	7,458.9450	**5430.3399**
7	**1.6711**	2.5902	**1.9635**	**5,274.6463**	7,632.7029	**5641.2444**
8	**1.9163**	2.6175	**1.9689**	**5,350.2330**	7,829.8352	**5948.7154**
9	**1.9649**	2.7587	**1.9749**	**5,353.7903**	7,986.5011	**5976.1547**
10	**1.9809**	2.8478	**2.0412**	**5,713.3339**	8,051.9947	**6240.8634**
11	**1.9975**	2.8738	**2.0557**	**5,758.4859**	8,114.1258	**6316.8534**
12	**2.0234**	2.8808	**2.0731**	**6,248.8423**	8,454.1336	**6626.1592**
13	2.2615	3.0187	2.0852	6,691.2576	8,626.6082	6687.2181
14	2.2837	3.0473	2.1016	6,799.8298	9,686.8360	6720.4324
15	2.3124	3.1867	2.1505	6,936.5144	9,788.7525	6918.9744
16	2.3790	3.3717	2.2022	6,949.0603	9,842.7553	7083.8602
17	2.6283	3.6827	2.2048	7,808.9009	10,981.2925	7109.1353
18	2.6644	3.8045	2.2324	8,826.8160	11,741.7673	7222.8883

Table 3 The average precision of monthly forecasting of inflow of Chinese tourists to the US. MAPE and RMSE are averaged across all predicted data during the period August 2013-September 2017, while model estimation is based on the data from the period January 1996-July 2013.

P.R.China	MAPE (%)			RMSE		
Horizon	NNeSTSM-HP	NNeSTSM-MA	NehM-STSM	NNeSTSM-HP	NNeSTSM-MA	NehM-STSM
1	2.1939	2.6700	1.5890	3,389.4265	3,867.8937	2512.5841
2	2.2354	2.7582	2.1122	3,535.8994	5,363.7645	2820.0064
3	**2.3853**	2.9167	**2.4317**	3,608.4120	6,167.2981	4287.4174
4	**2.5095**	3.2158	**2.8817**	3,679.6287	6,960.3408	5119.7475
5	**2.8493**	3.4330	**3.1640**	3,851.8719	7,357.0434	5555.2003
6	**2.8788**	3.6580	**3.4916**	4,464.0106	7,685.4256	5571.5591
7	**3.0546**	4.5565	**4.1331**	5,080.0699	8,326.3558	6337.3278
8	**3.6452**	4.9174	**4.1675**	5,406.6520	8,777.0933	6715.0477
9	**4.0254**	4.9781	**4.2239**	5,492.1599	9,142.2132	6741.8255
10	4.3749	5.0052	4.2676	5,556.7633	10,562.9857	7160.4687
11	4.5822	5.5689	4.3154	6,458.7721	12,049.3078	7512.0370
12	4.6617	5.6944	4.3629	9,245.5575	12,343.0974	7630.8765
13	4.8025	6.1542	4.4099	9,719.7594	12,744.8141	9673.1791
14	4.8565	6.8230	4.4263	10,366.2691	14,315.0753	10004.0591
15	5.8348	7.6449	4.4883	12,210.8285	16,494.3540	10024.4359
16	6.0910	8.7256	4.5042	13,664.4354	17,081.6246	10265.6192
17	6.1872	9.1358	4.5495	15,102.8313	20,231.3794	10375.7248
18	6.2882	10.2183	4.5550	15,812.8968	20,998.1905	10801.0503

Table 4 The average precision of monthly forecasting of inflow of Canadian tourists to the US. MAPE and RMSE are averaged across all predicted data during the period August 2013-September 2017, while model estimation is based on the data from the period January 1996-July 2013.

CANADA	MAPE (%)			RMSE		
Horizon	NNeSTSM-HP	NNeSTSM-MA	NehM-STSM	NNeSTSM-HP	NNeSTSM-MA	NehM-STSM
1	1.9035	2.0288	1.5596	29,574.0551	29,115.2496	23348.4713
2	1.9213	2.0366	1.5984	31,639.8449	32,423.3141	24636.8265
3	1.9998	2.0508	1.6360	32,997.5614	33,268.1662	24795.3656
4	2.0176	2.0985	1.6753	34,349.9232	37,737.8413	24876.6925
5	2.1590	2.2578	1.7088	34,652.0709	38,551.6398	25501.5102
6	2.1766	2.4782	1.7523	34,838.0449	40,927.5715	25884.5410
7	2.1797	2.5653	1.7655	36,389.6919	46,293.5134	26045.4341
8	2.2958	2.8336	1.7879	38,467.9057	53,846.6558	26216.5628
9	2.4023	2.9751	1.8135	42,776.4385	54,351.7902	26603.7664
10	2.5649	3.2464	1.8473	44,424.6116	55,052.8761	27695.4449
11	2.6107	3.4492	1.8780	44,483.5258	56,376.6186	29288.3842
12	2.7096	3.4499	1.9169	46,719.3535	59,543.0840	29773.2073
13	2.7706	3.6082	1.9323	46,869.1387	59,832.5781	31736.4468
14	2.9847	3.8336	1.9560	48,633.3919	61,402.9161	32161.7312
15	3.2304	4.1664	1.9935	50,546.9690	62,518.2238	32353.1747
16	3.4763	4.2384	1.9936	55,964.3055	66,041.3895	33043.6654
17	3.9160	4.3333	2.0053	69,943.1255	66,111.7145	33091.2679
18	4.7323	4.5588	2.0283	117,251.7355	70,288.0321	33923.5333

Table 5 The average precision of monthly forecasting of inflow of Mexican tourists to the US. MAPE and RMSE are averaged across all predicted data during the period August 2013-September 2017, while model estimation is based on the data from the period January 1996-July 2013.

MEXICO	MAPE (%)			RMSE		
Horizon	NNeSTSM-HP	NNeSTSM-MA	NehM-STSM	NNeSTSM-HP	NNeSTSM-MA	NehM-STSM
1	2.0551	3.1615	1.7986	23,008.9286	35,896.4678	25470.5902
2	2.1493	3.1794	1.8554	30,034.8306	45,076.1205	26308.8634
3	2.2997	3.6235	2.3909	32,120.5691	49,137.0452	28908.4991
4	2.3816	3.6724	3.5128	32,689.2784	51,805.6269	45942.3311
5	2.3954	3.7165	3.8835	35,360.0412	54,152.3174	51145.9735
6	2.4068	6.1008	4.1627	37,918.8539	74,973.5001	56300.8959
7	2.5992	6.5296	4.2037	38,737.2888	80,005.6105	59711.6139
8	2.6431	6.9635	4.2291	39,970.9958	93,468.5149	61326.6282
9	2.6603	7.1458	4.4652	41,492.9709	98,001.1533	63203.4026
10	2.7547	7.1770	4.7197	43,861.5262	102,553.8870	64230.1731
11	2.9492	7.2857	4.8740	45,512.4265	103,310.2356	70535.8700
12	2.9575	7.3130	5.0981	46,122.7767	105,057.1264	71701.7775
13	3.0117	7.7906	5.1982	46,799.1201	105,735.4548	72835.4986
14	3.1128	7.8629	5.2329	47,804.7792	107,459.8577	73278.3120
15	3.2467	7.8649	5.3746	48,535.5247	110,370.2890	78453.6638
16	3.3036	8.1077	5.5123	49,214.1087	114,738.5518	78641.1904
17	3.5934	8.1079	5.8336	50,539.1630	116,850.5917	81824.1781
18	3.6229	8.1335	5.8975	54,686.8468	119,028.1019	88882.9838

Table 6 The average precision of monthly forecasting of inflow of French tourists to the US. MAPE and RMSE are averaged across all predicted data during the period August 2013-September 2017, while model estimation is based on the data from the period January 1996-July 2013.

FRANCE	MAPE (%)			RMSE		
Horizon	NNeSTSM-HP	NNeSTSM-MA	NehM-STSM	NNeSTSM-HP	NNeSTSM-MA	NehM-STSM
1	2.0968	2.6193	1.6697	2,204.1445	2,583.0345	1417.1331
2	2.1712	3.3467	1.8777	2,321.2121	3,559.6996	1435.7498
3	2.2151	3.6270	1.8829	2,441.6981	4,545.7766	1566.7104
4	2.2767	3.7776	1.9588	2,478.8577	4,770.9112	1626.7368
5	2.3220	5.2181	2.0163	3,017.5703	4,847.1334	1942.2822
6	2.5546	5.3940	2.0425	3,054.1489	5,440.8341	2020.2504
7	2.6189	5.4629	2.0683	3,187.0396	5,883.8394	2171.6906
8	2.7427	5.6700	2.1146	3,240.0692	6,090.0635	2208.6878
9	2.8423	5.7421	2.1183	3,460.5369	6,735.7209	2353.9587
10	2.8521	5.7862	2.1690	3,502.2232	7,284.6118	2384.3391
11	3.0307	6.2567	2.2071	3,546.2541	8,493.6410	2518.1650
12	3.2129	6.3154	2.3341	4,547.2265	8,643.9093	2612.9452
13	3.2134	6.3256	2.4961	4,788.6029	9,078.5282	2864.3710
14	3.4172	6.9927	2.5178	4,809.2516	10,274.5840	2994.9699
15	3.5129	7.0585	2.5608	5,351.4803	10,315.5725	3220.0646

16	3.6808	8.1430	2.6175	5,949.9461	10,368.8115	3223.7053
17	3.8886	8.2036	2.6236	6,418.1043	10,462.3922	3257.1460
18	4.0212	8.2543	2.6317	6,530.2179	10,671.9451	3288.2015

Table 7 The average precision of monthly forecasting of inflow of British tourists to the US. MAPE and RMSE are averaged across all predicted data during the period August 2013-September 2017, while model estimation is based on the data from the period January 1996-July 2013.

UK	MAPE (%)			RMSE		
Horizon	NNeSTSM-HP	NNeSTSM-MA	NehM-STSM	NNeSTSM-HP	NNeSTSM-MA	NehM-STSM
1	2.0125	2.0136	1.6613	5,905.0835	6,811.1439	3798.5859
2	2.0292	2.0192	1.6702	6,394.6941	7,184.9834	3992.1153
3	2.1592	2.0834	1.7447	7,055.4306	8,102.3625	4006.7844
4	2.1748	2.1805	1.8177	7,914.8472	8,925.2220	5910.4819
5	2.3482	2.2493	1.9077	8,553.7269	9,114.8483	6543.1342
6	2.6110	2.4806	1.9170	8,553.8564	9,160.5909	6561.7763
7	2.6127	2.6586	1.9328	9,470.1553	9,992.9597	6624.8191
8	2.7743	2.9626	1.9649	9,484.3761	10,021.0201	6716.7608
9	2.8075	3.0014	1.9897	9,522.9954	10,109.8395	6731.3691
10	2.8297	3.7035	2.0413	10,405.7139	11,812.6566	7195.2826
11	2.8436	3.8187	2.0434	10,583.7699	11,866.8348	7508.1648
12	3.1550	3.9078	2.1550	10,797.7889	12,275.2218	7527.9648
13	3.5197	4.0512	2.1806	12,552.6999	12,801.4114	7602.9052
14	3.7874	4.1160	2.1817	12,601.5293	13,098.4995	7738.9987
15	3.9738	4.2072	2.1918	13,862.9409	14,147.0197	8147.0584
16	4.0694	4.2164	2.2299	14,115.8330	15,423.6550	8239.5793
17	4.3471	5.1342	2.2487	16,254.6417	16,217.2473	8309.2794
18	5.2968	5.6525	2.2882	16,629.8387	16,722.6244	8333.2153

Note: MAPE is Mean Average Absolute Percentage Error; RMSE is Root Mean Square Error; NNeSTSM-HP is the Neural Network enhanced STSM model with HP filter; NNeSTSM-MA is the Neural Network enhanced STSM model with Moving Average as the trend filter; NehM-STSM is the Neural Network enhanced hidden Markovian STSM model.

4. Conclusion

Modelling and predicting tourism data across short as well as long horizons are significantly influenced by the long-term trend element and strong recurrent seasonal element incorporated in tourism data. Building on the research by [3, 14, 27, 29], the present study puts forth a new hybrid model comprising neural network and multiplicative hidden Markovian processes. The low-pass Hodrick-Prescott filter is employed for explicit breakdown of the original tourism inflow data. This process is confirmed as a stationary seasonal process because it is conditional upon the stationarity and seasonality of the seasonal element. The original tourism series divided by the trend element gives the seasonal element. Estimation of a three-layer autoregressive neural network with ten hidden neurons and of a multiplicative hidden Markovian process is respectively undertaken based on the trend element and the seasonal element. The final forecasting outcome of the tourism series is the sum of the outputs of the neural network and multiplicative hidden Markovian process. The advantages of the new proposed NehM-STSM model are twofold: 1) as the traditional econometrics model, NehM-STSM assumes a time-variant trend with a strong seasonal pattern in the tourism demand data; however, NehM-STSM assumes the non-linearity of the two component and explicitly obtain them and model them separately. The tailor-made mechanism provides the NehM-STSM outperformance; 2) NehM-STSM considers the factors that impact the seasonal patterns by the abstracted format of a persistence replicative component, a jump component capturing the impact event, an event amplitude component and a random error term. Such structure provides a generic framework of all possible

impact factors: regardless the factors, their impact on the seasonality reflects on one of the abstracted components. Apparently, the structure of the NehM-STSM model significantly increases the time and space complexity during the training process and requires relatively large volume of training data and the high-end computing facility in the employment of the proposed model. The empirical studies of this work include the data of tourism inflow from twelve major source markets to the US up to 18 forecasting horizons by the NehM-STSM, NNeSTSM-HP, NNeSTSM-MA, and the SARIMA models. According to the out-of-sample forecasting results, NehM-STSM has a higher performance than NNeSTSM-HP and NNeSTSM-MA. On average, the proposed NehM-STSM model performs slightly better (i.e., less than 0.5%) to the NNeSTSM-HP model in forecasting horizon of one to five months ahead. However, in the horizon more than five months, the proposed NehM-STSM model outperforms the NNeSTSM-HP model by 1% up to 3%, and NNeSTSM-MA more than 5%. The good forecasting results are mainly due to the hidden Markovian processes effectively capture the seasonal patterns of the tourism demand. The empirical results in twelve major markets across 20 years show that a model structure that contains the ANN and the multiplicative hidden Markovian process is capable to well capture the tourism demand changes with strong time-variant seasonal patterns. Such model structure can be easily applied in forecasting time series in other areas, which contains a trend and a cyclical pattern. In future research, the NehM-STSM model should be refined to deal with data structural break changes.

Acknowledgements

This research is partially supported by the National Social Science Fund of China (Grant No. 17BJY194) and Philosophy and Social Science Key project development plan in Henan University (Grant No. 2019ZDXM016).

References

[1] R. Butler, “Seasonality in Tourism: Issues and Implications,” in *Seasonality in Tourism*, Oxford, Pergamon, 2001, p. 5–21.

[2] C. Lim and M. McAleer., “Monthly Seasonal Variations: Asian Tourism to Australia,” *Annals of Tourism Research,* vol. 28, no. 1, p. 68–82, 2001.

[3] J. L. Chen, G. Li, D. C. Wu and S. Shen, “Forecasting Seasonal Tourism Demand Using a Multiseries Structural Time Series Method,” *Journal of Travel Research*, vol. 58, no. 1, pp. 1-12, 2017.

[4] J. Zhang, X. Zhu, J. Feng and Y. Yang, “Finding community of brain networks based on artificial bee colony with uniform design,” *Multimedia Tools and Applications,* vol. 78, p. 33297–33317, 2019.

[5] J. Zhang, L. Tang, B. Liao, X. Zhu and F.-X. Wu, “Finding Community Modules of Brain Networks Based on PSO with Uniform Design,” *BioMed Research International,* 2019.

[6] Y. Yao, Y. Cao, X. Ding, J. Zhai, J. Liu, Y. Luo, S. Ma and K. Zou, “A paired neural network model for tourist arrival forecasting,” *Expert Systems with Applications,* vol. 114, pp. 588-614, December 2018.

[7] J. H. Kim, “Forecasting Monthly Tourist Departures from Australia,” *Tourism Economics,* vol. 5, no. 3, p. 277–91, 1999.

[8] D. R.Osborna, S. Heravib and C. R. Birchenhallc, “Seasonal Unit Roots and Forecasts of Two-Digit European Industrial Production,” *International Journal of Forecasting,* vol. 15, p. 27–47, 1999.

[9] E. Ghysels and D. R. Osborn, The Econometric Analysis of Seasonal Time Series, Cambridge: Cambridge University Press., 2001.

[10] H. Song, G. Li, S. F. Witt and G. Athanasopoulos, “Forecasting Tourist Arrivals Using Time-Varying Parameter Structural Time-Series Models,” *International Journal of Forecasting,* vol. 27, p. 855–69, 2011.

[11] D. Alleyne, “Can Seasonal Unit Root Testing Improve the Forecasting Accuracy of Tourist Arrivals,” *Tourism Economics,* vol. 12, p. 45–64, 2006.

[12] N. Kulendran and S. F. Witt, “Forecasting the Demand for International Business Tourism,” *Journal of Travel Research,* vol. 41, p. 265–271, 2003.

[13] C.-O. Oh and B. J. Morzuch, “Evaluating Time-Series Models to Forecast the Demand for Tourism in Singapore,” *Journal of Travel Research,* vol. 43, p. 404–13, 2005.

[14] A. Harvey and P. Todd, “Forecasting economic time series with structural and Box-Jenkins Model: A Case Study,” *Journal of Business & Economic Statistics,* pp. 299-307, 1983.

[15] S. C. Kon and L. W. Turner, “Neural Network Forecasting of Tourism Demand,” *Tourism Economics,* vol. 11, p. 301–28, 2005.

[16] M. Muysal and M. S. E. Roubi, “Artificial Neural Networks versus Multiple Regression in Tourism Demand Analysis,” *Journal of Travel Research,* vol. 38, pp. 111-118, 1999.

[17] R. Law, “Back-propagation learning in improving the accuracy of neural network-based tourism demand forecasting,” *Tourism Management,* vol. 21, no. 4, p. 331–340, 2000.

[18] C. Burger, M. Dohnal, M. Kathrada and R. Law, “A practitioner’s guide to time series methods for tourism demand forecasting – a case study of Durban, South Africa,” *Tourism Management,* p. 403–409, 2001.

[19] O. Claveria and S. Torra, “Forecasting tourism demand to Catalonia: Neural networks vs. time series models,” *Economic Modelling,* vol. 36, p. 220–228, 2014.

[20] H. Hassani, E. S. Silva, N. Antonakakis, G. Filis and R. Gupta, “Forecasting accuracy evaluation of tourist arrivals,” *Annals of Tourism Research,* vol. 63, p. 112–127, 2017.

[21] P.-F. Pai, K.-C. Hung and K.-P. Lin, “Tourism demand forecasting using novel hybrid system,” *Expert Systems with Applications,* vol. 41, p. 3691–3702, 2014.

[22] W. Briec, K. Kerstens, D. Prior and I. Van de Woestyne, “Testing general and special Färe-Primont indices: A proposal for public and private sector synthetic indices of European regional expenditures and tourism,” *European Journal of Operational Research,* vol. 271, no. 2, pp. 756-768, December 2018.

[23] G. S. Atsalakis, I. G. Atsalaki and C. Zopounidis, “Forecasting the success of a new tourism service by a neuro-fuzzy technique,” *European Journal of Operational Research,* vol. 268, no. 2, pp. 716-727, July 2018.

[24] S. Cang and H. Yu, “A combination selection algorithm on forecasting,” *European Journal of Operational Research,* vol. 234, no. 1, pp. 127-139, April 2014.

[25] G. P. Zhang and M. Qi, “Neural network forecasting for seasonal and trend time series,” *European Journal of Operational Research,* p. 501–514, 2005.

[26] S. Patil, H. Tantau and V. Salokhe, “Modelling of tropical greenhouse temperature by autoregressive and neural network models,” *Biosystems Engineering,* p. 423–431, 2008.

[27] Y. Yao, J. Zhai, Y. Cao, X. Ding, J. Liu and Y. Luo, “Data analytics enhanced component volatility model,” *Expert Systems with Applications,* vol. 84, pp. 232-241, 2017.

[28] Y. Cao, Y. Li, S. Coleman, A. Belatreche and T. M. McGinnity, “Adaptive Hidden Markov Model With Anomaly States for Price Manipulation Detection,” *IEEE Transactions on Neural Networks and Learning Systems,* vol. 26, no. 2, pp. 318-330, Feburary 2015.

[29] M. Augustyniak, L. Bauwens and A. Dufays, “A new approach to volatility modeling: the factorial hidden Markov volatility model,” *Journal of Business & Economic Statistics,* p. DOI: 10.1080/07350015.2017.1415910, 2018.

[30] R. D.F.Harris, E. Stoja and F. Yilmaz, “A cyclical model of exchange rate volatility,” *Journal of Banking and Finance,* vol. 35, pp. 3055-3064, 2011.

[31] Y. Tian, G. J. Huffman, R. F. Adler, L. Tang, M. Sapiano, V. Maggioni and H. Wu, “Modeling errors in daily precipitation measurements: Additive or multiplicative?,” *Geophysical Research Letters,* vol. 40, no. 10, pp. 2060-2065, 2013.

[32] N. Hautsch, “Capturing common components in high-frequency financial time series: A multivariate stochastic multiplicative error model,” *Journal of Economic Dynamics and Control,* vol. 32, no. 12, pp. 3978-4015, 2008.

[33] M. Lanne, “A mixture multiplicative error model for realized volatility,” *Journal of Financial Econometrics,* pp. 594-616, 2006.

[34] R. Engle, “New frontiers for arch models,” *Journal of Applied Econometrics,* pp. 425-446, 28 October 2002.

[35] R. F.Engle and G. M.Gallo, “A multiple indicators model for volatility using intra-daily data,” *Journal of Econometrics,* vol. 131, pp. 3-27, March–April 2006.

[36] G. M.Gallo and EdoardoOtranto, “Forecasting realized volatility with changing average levels,” *International Journal of Forecasting,* p. 620{634, 2015.

[37] F. Petropoulos, S. Makridakis, V. Assimakopoulos and K. Nikolopoulos, “‘Horses for Courses’ in demand forecasting,” *European Journal of Operational Research,* vol. 237, p. 152–163, 2014.

[38] T. Rydén, T. Teräsvirta and S. Åsbrink, “Stylized facts of daily return series and the hidden Markov model,” *Journal of Applied Econometrics,* pp. 217-244, 21 December 1998.

[39] P. Guo, Z. Miao, X.-P. Zhang, Y. Shen and S. Wang, “Coupled Observation Decomposed Hidden Markov Model for Multiperson Activity Recognition,” *IEEE Transactions on Circuits and Systems for Video Technology,* vol. 22, no. 9, pp. 1306-1320, September 2012.

[40] A. G. Assaf, G. Li, H. Song and M. G. Tsionas, “Modeling and forecasting regional tourism demand using the Bayesian GVAR (BGVAR) model,” *Journal of Travel Research,* p. in press, 2018.

[41] R. Hodrick and E. C. Prescott, “Postwar US business cycles: an empirical investigation,” *Journal of Money, Credit and Banking,* pp. 1-16, 1997.

[42] J. H. Stock and M. W. Watson, “Forecasting Inflation,” *Journal of Monetary Economics,* p. 293–335, 1999.

[43] T. McElroy, “Exact Formulas for the Hodrick-Prescott Filter,” *Econometrics Journal,* p. 209–217, 2008.

[44] J. H. Stock and M. W. Watson, “Dynamic Factor Models, Factor-Augmented Vector Autoregressions, and Structural Vector Autoregressions in Macroeconomics,” in *Handbook of Macroeconomics,* ELSEVIER, 2016, pp. Volume 2, 415–525.

[45] W. A. Fuller, Introduction to Statistical Time Series, Wiley, 1976.

[46] M. Baxter and R. G. King, “Measuring Business Cycles Approximate Band-Pass Filters for Economic Time Series,” *Review of Economics and Statistics,* pp. 575-593, 1999.

[47] M. O. Ravn and H. Uhlig, “On adjusting the Hodrick–Prescott filter for the frequency of observations,” *Review of Economics and Statistics,* pp. 371-375, 2002.

[48] W. Kristjanpoller and M. C. Minutolo, “Forecasting volatility of oil price using an artificial neural network-GARCH model,” *Expert Systems With Applications,* vol. 65, p. 233–241, 2016.

[49] G. Mustafaraj, G. Lowry and J. Chen, “Prediction of room temperature and relative humidity by autoregressive linear and nonlinear neural network models for an open office,” *Energy and Buildings,* p. 1452–1460, 2011.

[50] H. T. Siegelmann, Bill G. Horne and C. L. Giles, “Computational capabilities of recurrent NARX neural networks,” *IEEE Transactions on Systems, Man, and Cybernetics, Part B (Cybernetics),* pp. 208 - 215, 1997.

[51] M. T. Hagan and M. B. Menhaj., “Training feedforward networks with the Marquardt algorithm,” *IEEE transactions on Neural Networks,* pp. 989-993, 1994.

[52] J. D. Hamilton, “A New Approach to the Economic Analysis of Nonstationary Time Series and the Business Cycle,” *Econometrica,* vol. 57, no. 2, pp. 357-384, 1989.

[53] J. D. Hamilton, Time series analysis, New Jersey: Princeton University Press, 1994.

[54] T. G. Andersen and T. Bollerslev, "Heterogeneous information arrivals and return volatility dynamics: Uncovering the long-run in high frequency returns," *The Journal of Finance,* vol. 52, no. 3, pp. 975-1005, 1997.

[55] S. Sun, Y. Wei, K.-L. Tsui and S. Wang, "Forecasting tourist arrivals with machine learning and internet search index," *Tourism Management,* p. in press, 2019.

[56] S. K. Wan and H. Song, "Forecasting turning points in tourism growth," *Annals of Tourism Research,* vol. 72, pp. 156-167, 2018.

[57] E. Sirimal Silva, Z. Ghodsi, M. Ghodsi, S. Heravi and H. Hassani, "Cross country relations in European tourist arrivals," *Annals of Tourism Research,* vol. 63, pp. 151-168, 2017.

[58] X. Li, B. Pan, R. Law and X. Huang, "Forecasting tourism demand with composite search index," *Tourism Management,* vol. 59, pp. 57-66, 2017.

[59] B. Pan and Y. Yang, "Forecasting Destination Weekly Hotel Occupancy with Big Data," *Journal of Travel Research,* vol. 56, pp. 957-970, 2016.

[60] L. Wu and G. Cao, "Seasonal SVR with FOA algorithm for single-step and multi-step ahead forecasting in monthly inbound tourist flow," *Knowledge-Based Systems,* pp. 157-166, 2016.

[61] RobertoRivera, "A dynamic linear model to forecast hotel registrations in Puerto Rico using Google Trends data," *Tourism Management,* vol. 57, pp. 12-20, 2016.

[62] U. Gunter and I. Onder, "Forecasting international city tourism demand for Paris: Accuracy of uni- and multivariate models employing monthly data," *Tourism Management,* vol. 46, pp. 123-135, 2015.

[63] P. F.Bangwayo-Skeete and R. W.Skeete, "Can Google data improve the forecasting performance of tourist arrivals? Mixed-data sampling approach," *Tourism Management,* vol. 46, pp. 454-464, 2015.

[64] H. Song, B. Z. Gao and V. S. Lin, "Combining statistical and judgmental forecasts via a web-based tourism demand forecasting system," *International Journal of Forecasting,* vol. 29, pp. 295-310, 2013.

[65] J. Shahrabi, E. Hadavandi and S. Asadi, "Developing a hybrid intelligent model for forecasting problems: Case study of tourism demand time series," *Knowledge-Based Systems,* vol. 43, pp. 112-122, May 2013.

[66] C.-F. Chen, M.-C. Lai and C.-C. Yeh, "Forecasting tourism demand based on empirical mode decomposition and neural network," *Knowledge-Based Systems,* vol. 26, pp. 281-287, 2012.

[67] R. Fildes, Y. Wei and S. Ismail, "Evaluating the forecasting performance of econometric models of air passenger traffic flows using multiple error measures," *International Journal of Forecasting,* vol. 27, p. 902–922, 2011.

[68] F.-L. Chu, "Forecasting tourism demand with ARMA-based methods," *Tourism Management,* vol. 30, p. 740–751, 2009.

[69] G. Athanasopoulos and R. J.Hyndman, "Modelling and forecasting Australian domestic tourism," *Tourism Management,* vol. 29, pp. 19-31, 2008.

[70] K. K. Wong, H. Song, S. F. Witt and D. C. Wu, "Tourism forecasting: To combine or not to combine?," *Tourism Management,* vol. 28, p. 1068–1078, 2007.

[71] N. Kulendran and K. K. F. Wong, "Modelling Seasonality in Tourism Forecasting," *Journal of Travel Research,* vol. 44, p. 163–70, 2005.

[72] J. Preez and S. F.Witt, “Univariate versus multivariate time series forecasting: an application to international tourism demand,” *International Journal of Forecasting,* vol. 19, pp. 435-451, September 2003.

[73] S.-X. Lv, L. Peng and L. Wang, “Stacked autoencoder with echo-state regression for tourism demand forecasting using search query data,” *Applied Soft Computing Journal,* vol. 73, p. 119–133, 2018.

[74] W.-C. Hong, Y. Dong, L.-Y. Chen and S.-Y. Wei, “SVR with hybrid chaotic genetic algorithms for tourism demand forecasting,” *Applied Soft Computing,* vol. 11, no. 2, pp. 1881-1890, 3 2011.

[75] R. Law and N. Au, “A neural network model to forecast Japanese demand for travel to Hong Kong,” *Tourism Management,* p. 89–97, 1999.

[76] W. Kristjanpoller, A. Fadic and M. C. Minutolo, “Volatility forecast using hybrid Neural Network models,” *Expert Systems with Applications,* p. 2437–2442, 2014.

Appendix

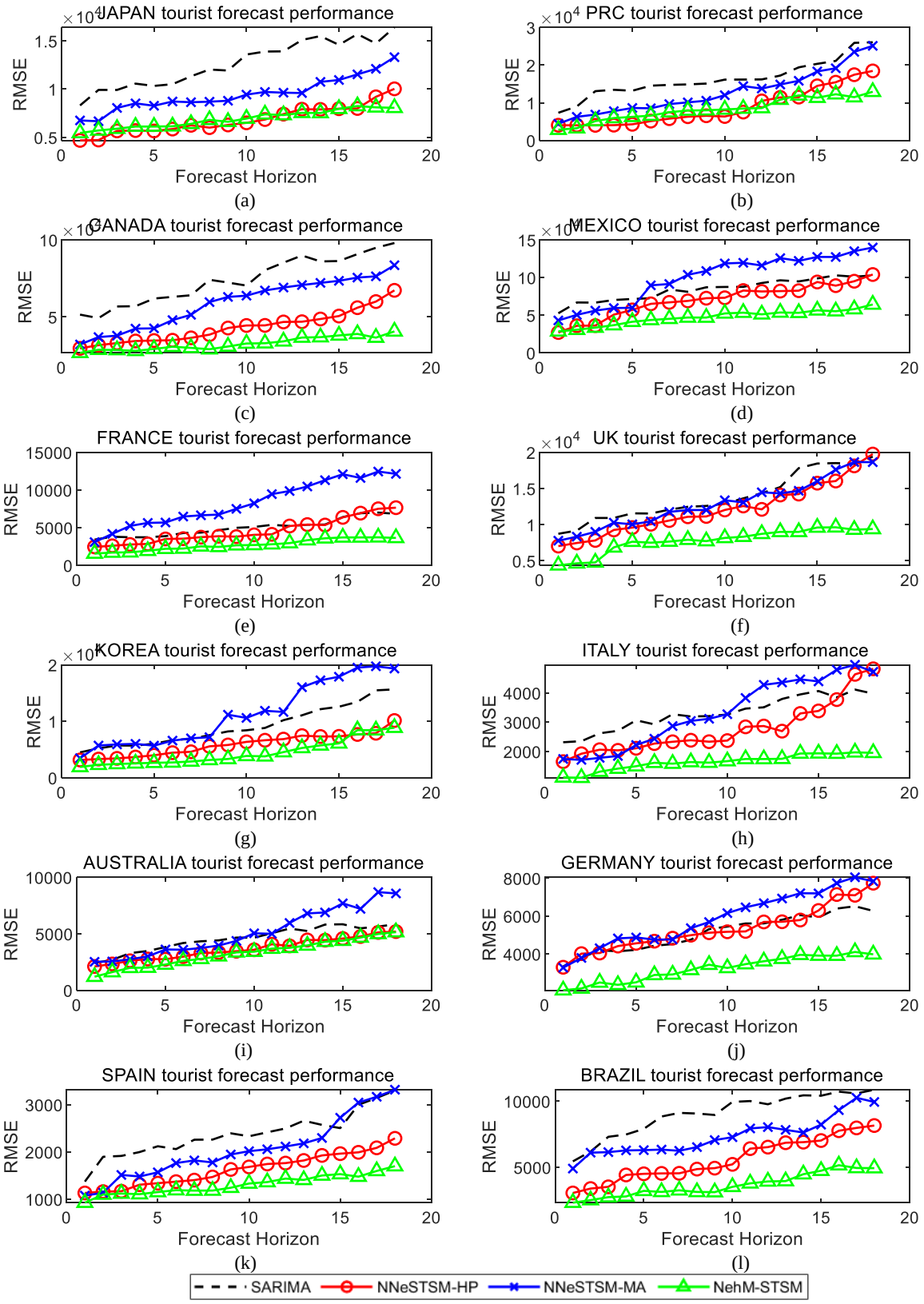

Appendix Figure 1 Forecasting error measures of **RMSE** achieved by the SARIMA, NNeSTSM-HP, NNeSTSM-MA and NehM-STSM models regarding tourist inflows from twelve source markets (Japan, Mainland China, Canada, Mexico, France, UK, Korea, Italy, Australia, Germany, Spain, and Brazil). Model estimation is based on data from the period January 1996-December 2009, which are summarised in the graphs to ensure clarity. The forecasting outcomes cover the period January 2010-September

2017. NehM-STSM = Neural Network-enhanced hidden Markov Structural Time Series Model; NNeSTSM-HP = Neural Network-enhanced STSM model with HP filter; NNeSTSM-MA = Neural Network-enhanced STSM model with Moving Average as the trend filter.

Appendix Table 1 This table shows the average accuracy of monthly forecasts of US tourist arrivals from ITALY. The MAPE and RMSE are average values across all forecasted data from Aug 2013 to Sep 2017. The models are all estimated by the data from Jan 1996 to Jul 2013.

ITALY	MAPE (%)			RMSE		
Horizon	NNeSTSM-HP	NNeSTSM-MA	NehM-STSM	NNeSTSM-HP	NNeSTSM-MA	NehM-STSM
1	2.0760	2.2960	1.5638	1,475.6624	1,457.7917	936.4578
2	2.1643	2.2975	1.6673	1,666.8365	1,550.6151	980.6446
3	2.4231	2.4264	1.6917	1,771.6161	1,586.2061	1132.4206
4	2.5114	2.4301	1.8404	1,788.0513	1,635.6921	1229.8841
5	2.5947	2.5749	1.8460	1,813.4666	1,995.6738	1298.3736
6	2.8404	2.5902	1.8594	1,917.3266	2,094.8811	1345.3443
7	2.8780	2.7442	1.9749	2,044.4124	2,466.9727	1375.1717
8	2.9147	3.3665	2.0370	2,054.7212	2,547.7043	1410.9643
9	2.9329	3.5887	2.0592	2,074.7729	2,750.9733	1457.2117
10	3.0640	3.6322	2.0601	2,134.1112	2,859.2173	1470.0406
11	3.1256	3.7910	2.0954	2,418.3283	3,421.4189	1477.8052
12	3.1793	4.1297	2.0975	2,430.2504	3,676.2009	1482.2882
13	3.2600	4.3187	2.1138	2,433.6272	3,807.4520	1555.1989
14	3.2896	4.4406	2.1350	2,797.2310	3,862.3840	1617.5904
15	4.0717	4.8030	2.1453	2,917.3847	3,900.5534	1633.5497
16	4.1003	4.9981	2.2125	3,357.8388	4,175.0139	1685.3512
17	4.4225	5.6311	2.2724	3,897.4073	4,180.4292	1687.2069
18	5.1484	5.9064	2.3108	4,032.1618	4,204.3810	1703.0690

Appendix Table 2 This table shows the average accuracy of monthly forecasts of US tourist arrivals from SPAIN. The MAPE and RMSE are average values across all forecasted data from Aug 2013 to Sep 2017. The models are all estimated by the data from Jan 1996 to Jul 2013.

SPAIN	MAPE (%)			RMSE		
Horizon	NNeSTSM-HP	NNeSTSM-MA	NehM-STSM	NNeSTSM-HP	NNeSTSM-MA	NehM-STSM
1	2.0620	2.0070	1.6159	1,131.2550	967.7461	821.7475
2	2.2655	2.0861	1.6872	1,159.9743	969.5743	934.6483
3	2.2796	2.1114	1.7509	1,167.8067	1,299.0070	956.7833
4	2.4873	2.1931	1.7745	1,306.2908	1,334.5188	962.1861
5	2.5127	2.2924	1.9082	1,338.3505	1,396.7860	986.9406
6	2.5820	2.3603	1.9512	1,371.1106	1,538.6468	1000.8060
7	2.6814	2.6981	1.9829	1,403.6249	1,550.6383	1011.2027
8	2.8738	2.7678	2.1235	1,469.7818	1,553.7871	1032.6326
9	3.1616	2.7878	2.1507	1,629.6006	1,649.0506	1080.0721
10	3.3143	3.0014	2.1742	1,682.1278	1,698.8751	1175.0529
11	3.3900	3.8057	2.2708	1,744.6072	1,761.1165	1194.6776
12	3.4045	3.8778	2.2830	2,063.5352	1,808.4086	1257.2086
13	3.7876	3.8861	2.3353	2,419.1042	1,893.1316	1257.8672
14	3.9407	3.8905	2.3367	2,725.9535	2,011.4587	1286.2419
15	5.1572	4.0116	2.3691	2,913.4500	2,376.6354	1294.1468
16	5.7490	4.1130	2.4666	3,181.5540	2,568.4638	1300.0468
17	5.7636	4.1994	2.4931	3,286.3516	2,740.7787	1418.1323
18	6.3312	4.5619	2.5197	3,287.6573	2,776.1523	1431.9225

Appendix Table 3 This table shows the average accuracy of monthly forecasts of US tourist arrivals from KOREA. The MAPE and RMSE are average values across all forecasted data from Aug 2013 to Sep 2017. The models are all estimated by the data from Jan 1996 to Jul 2013.

KOREA	MAPE (%)			RMSE		
Horizon	NNeSTSM-HP	NNeSTSM-MA	NehM-STSM	NNeSTSM-HP	NNeSTSM-MA	NehM-STSM
1	2.0793	2.1199	1.6558	2,640.2352	3,046.9965	1702.7453
2	2.1052	3.8615	1.6922	2,952.5378	4,879.4001	2078.7106
3	2.1470	4.1527	1.7219	3,085.8545	4,984.1086	2103.7348
4	2.2451	4.2305	1.7904	3,086.3512	5,002.5364	2275.5735
5	2.4745	4.2319	1.9303	3,471.6760	5,128.7030	2284.5419
6	3.0370	4.6459	1.9890	3,804.4224	5,592.8176	2431.6917
7	3.6132	4.7867	2.2267	4,032.4997	6,136.6385	2458.5053
8	3.7898	5.2997	2.6138	4,650.4786	6,279.4104	2765.5148
9	3.8106	7.5102	2.7404	5,191.7739	9,398.1144	2951.8585
10	3.8585	7.5286	2.7462	5,511.4165	9,484.0720	3321.3011
11	3.8876	8.4528	2.7959	5,819.9610	10,094.5358	3322.3296
12	3.9205	9.0589	3.0722	5,879.5808	10,315.7880	3855.9122
13	3.9252	9.1615	3.1211	6,364.2125	13,809.4776	4485.9743
14	4.0039	9.3973	3.6093	6,407.3150	14,805.1213	4862.4039
15	4.3950	9.9553	3.9641	6,593.0796	16,049.2606	5433.6812
16	4.6872	10.4615	4.5859	6,869.8729	16,449.2499	7144.8775
17	5.0658	10.6986	4.7038	7,006.9979	16,760.7544	7232.0126
18	5.6340	10.7651	4.7583	8,701.1004	17,084.5424	7452.8607

Appendix Table 4 This table shows the average accuracy of monthly forecasts of US tourist arrivals from BRAZIL. The MAPE and RMSE are average values across all forecasted data from Aug 2013 to Sep 2017. The models are all estimated by the data from Jan 1996 to Jul 2013.

BRAZIL	MAPE (%)			RMSE		
Horizon	NNeSTSM-HP	NNeSTSM-MA	NehM-STSM	NNeSTSM-HP	NNeSTSM-MA	NehM-STSM
1	2.2335	2.5098	1.5046	3,057.5383	4,257.6484	1980.8455
2	2.6828	3.1460	1.6981	3,392.3893	5,259.9389	2144.6272
3	2.7026	3.1878	1.8322	3,521.7652	5,283.6159	2432.3179
4	2.8603	3.4739	1.8454	4,420.9312	5,399.7015	2515.2901
5	2.8874	3.6534	1.8569	4,506.7629	5,406.3148	2757.8516
6	2.9132	3.7979	1.8827	4,537.9710	5,574.7851	2786.7100
7	2.9218	3.8081	2.0213	4,545.9499	5,634.5468	2794.9607
8	2.9962	3.8916	2.0982	4,863.4487	5,654.2005	2795.5737
9	3.0359	4.1216	2.2240	4,935.2503	6,305.7624	2820.4368
10	3.0871	4.5922	2.2583	5,222.5648	6,567.7108	3052.5253
11	3.1031	4.6884	2.3989	6,409.7712	6,625.3523	3156.1360
12	3.2811	4.7335	2.4131	6,524.7034	6,719.7297	3284.5918
13	3.3392	5.0993	2.4173	6,857.0126	6,893.2053	3557.1128
14	4.6565	5.1042	2.4749	7,413.8218	6,911.0253	3767.7148
15	5.0524	5.1769	2.4781	7,822.6411	7,187.5633	4060.7292
16	5.3771	5.3796	2.4885	9,764.8979	8,337.4461	4333.3787
17	6.0188	5.4892	2.6065	10,977.9553	8,693.2951	4338.6418
18	8.5497	5.7705	2.6280	15,743.3030	8,827.6983	4412.1274

Appendix Table 5 This table shows the average accuracy of monthly forecasts of US tourist arrivals from GERMANY. The MAPE and RMSE are average values across all forecasted data from Aug 2013 to Sep 2017. The models are all estimated by the data from Jan 1996 to Jul 2013.

GERMANY	MAPE (%)			RMSE		
Horizon	NNeSTSM-HP	NNeSTSM-MA	NehM-STSM	NNeSTSM-HP	NNeSTSM-MA	NehM-STSM
1	2.0232	2.0899	1.5711	2,886.2685	2,814.0082	1757.3587
2	2.0819	2.0990	1.6871	3,355.7972	3,240.0784	1857.4898
3	2.0951	2.1730	1.6981	3,677.2995	3,761.6868	2083.8911
4	2.0962	2.2608	1.7097	3,690.3158	4,086.0665	2088.4756
5	2.2106	2.2732	1.7423	4,077.4593	4,089.7474	2224.5407
6	2.2189	2.2953	1.7930	4,082.0890	4,112.9655	2435.5884
7	2.3521	2.2956	1.8259	4,176.1337	4,213.4900	2649.8362
8	2.3563	2.3728	1.8335	4,251.6155	4,736.7540	2731.9955
9	2.3769	2.5377	1.8845	4,350.0382	5,049.1387	2859.8656
10	2.3779	2.6588	1.9671	4,417.1725	5,282.7154	2860.6948
11	2.4945	2.7320	2.0156	4,695.4755	5,571.7511	2960.6886
12	2.6526	2.8772	2.0452	4,968.6968	5,641.2513	3269.3592
13	2.9490	2.9504	2.0770	4,992.0286	6,083.6366	3353.7597
14	3.0304	3.1776	2.1694	5,167.5828	6,146.0525	3360.1209
15	3.1270	3.3762	2.2009	5,358.2740	6,291.6163	3401.8004
16	3.2708	3.5396	2.2337	6,048.0195	6,560.1257	3492.5675
17	3.6697	3.9830	2.2431	6,385.2877	6,812.1865	3513.4731
18	3.7681	4.0417	2.2570	6,582.6340	6,880.3405	3515.0853

Appendix Table 6 This table shows the average accuracy of monthly forecasts of US tourist arrivals from AUSTRALIA. The MAPE and RMSE are average values across all forecasted data from Aug 2013 to Sep 2017. The models are all estimated by the data from Jan 1996 to Jul 2013.

AUSTRALIA	MAPE (%)			RMSE		
Horizon	NNeSTSM-HP	NNeSTSM-MA	NehM-STSM	NNeSTSM-HP	NNeSTSM-MA	NehM-STSM
1	2.0344	2.0963	1.5472	1,879.6087	2,203.7164	1027.8362
2	2.0633	2.1058	1.6562	1,976.2163	2,296.9482	1371.3213
3	2.1108	2.1105	1.7475	2,335.8330	2,487.9154	1656.2893
4	2.1143	2.3146	1.7491	2,403.0227	2,708.4169	1805.4700
5	2.1586	2.3347	1.7657	2,430.1701	3,024.3907	2003.2769
6	2.2065	2.3538	1.7798	2,655.8755	3,136.8702	2314.3030
7	2.2764	2.4584	1.9404	2,796.2365	3,148.3399	2388.1717
8	2.4465	2.7246	1.9918	2,823.3480	3,432.0916	2527.6011
9	2.6196	2.7901	2.1030	3,073.6260	3,888.0412	2908.8652
10	2.6956	3.7065	2.3810	3,134.7780	4,331.6185	2976.3895
11	2.7121	3.8835	2.6915	3,500.6858	4,414.2942	3157.5373
12	2.7825	5.0907	3.4248	3,564.7621	5,335.7646	3238.6334
13	3.1559	5.4759	3.4354	3,854.4347	5,855.3615	3486.6058
14	3.2456	5.5153	3.5845	3,870.5337	6,026.6730	3823.2241
15	3.4178	5.7663	3.6348	3,953.1031	6,466.3063	3982.7686
16	3.4516	6.1835	3.9519	3,970.5294	6,522.8144	4029.3722
17	3.7459	6.7793	4.0738	4,335.7868	7,241.5357	4212.5915
18	3.9772	6.7820	4.1080	4,429.4164	7,442.9502	4314.8553

Note: MAPE is Mean Average Absolute Percentage Error; RMSE is Root Mean Square Error; NNeSTSM-HP is the Neural Network enhanced STSM model with HP filter; NNeSTSM-MA is the Neural Network enhanced STSM model with Moving Average as the trend filter; NehM-STSM is the Neural Network enhanced hidden Markovian STSM model.

Appendix Table 7 Overview of studies related to tourism forecasting through traditional econometrics models published in the last decade; the frequency of data is provided per week (W), per month (M), quarterly (Q) and per year. Some machine learning models have also been included as benchmark models.

Paper	**Data Freq.**	**Methodology**	**variables**	**Finding and Limitation**
[55]	M	KELM, ELM, ANN, SVR, ARIMA, LSSVR	Tourist arrivals, Google search, Baidu search	KELM model with google and baidu search outperformed all others;
[56]	Q	LR HA, Naïve,	Tourist arrivals, GDP, Tourism price	Combining all information into a single model did not improve the performance; Combining logistic regression models can improve the predictive power;
[40]	Q	VAR, BGVAR,	Tourist arrivals, economic variable	BGVAR model captured the linkages between countries; Shock of economic variable has spill-over effects on other neighbouring countries;
[3]	Q	M-STSM	Tourist arrivals	Novel multivariate model capturing both the backward and forward inter-quarter dependencies to forecast the seasonal tourist arrival;
[57]	M	MSS, SSA, ARIMA, ETS	Tourist arrivals	Multivariate model with cross country relations improved the single model forecasting performance;
[58]	M	GDFM, PCA	Tourist arrivals	Index of search trend can improve the 1 and 4 week forecasting performance;
[59]	W	ARIMAX	Hotel demand, search queries, website traffic, weekly weather	ARMAX model with search queries and website traffic outperformed other models;
[60]	M	SFOASVR, SVR	Tourist arrivals	hybridized SFOASVR model outperformed the SARIMA, BPNN, SVR models significantly;
[61]	M	DLM, HW, SNAIVE	Hotel nonresident	Holt-Winter works best in short term forecasting; DLM is better in long term;
[62]	M	EC-ADLM, TVP VAR, BVAR,	Tourist arrivals, economic variable	No single model outperforms all others on all occasions;
[63]	M	AR-MIDAS	Tourist arrivals, Google trend data	Google searches on destination hotels and flights from source countries improved the forecasting performance;
[64]	Q	TDFS	Tourist arrivals	The web-based TDFS is proposed for stable, accurate and real-time tourism forecasting;
[65]	M	MGFFS	Tourist arrivals	The genetic algorithm based fuzzy system is significantly more accurate than other approaches;
[66]	M	EMD, BPNN	Tourist arrivals	EMD-BPNN model outperformed the single BPNN and ARIMA model in forecasting tourist arrival in HK;

[10]	Q	TVP-STSM	Tourist arrivals Economic variables	Novel time-varying STSM model with explanatory variable coefficients to forecast the quarterly tourist arrival;
[67]	Annual	ADLM, TVP, VAR	Air passengers economic variable	Pooled ADL models outperformed all other models; TVP models do not improve accuracy;
[68]	Q, M	ARMA, ARIMA, ARAR, ARFIMA	Tourist arrivals	ARFIMA outperformed all other ARMA-based models for both monthly and quarterly forecasting;
[69]	Q	LR, ETS, SS	Tourist arrivals Economic variables	All models outperformed official benchmark in short term but underperformed it in long term;
[70]	Q	SARIMA, DE, ECM, VC	Tourist arrivals	Combined models did not always outperform the best single forecasts but always outperformed the worst single model; Combined models are the safest choice;
[11]	Q	HEGY test	Tourism demand	HEGY test improve forecasts in all horizons except the high volatility cases;
[71]	Q	ARIMA	Tourism demand	HEGY test was not useful by the ARIMA1 and ARIMA14 results;
[13]	Q	Naïve I & II, LR, WM, ARIMA, SW,	Tourism demand	In-sample performance did not guarantee the out-of-sample performance; A combined model provided the best forecasting performance;
[12]	Q	STSM ARIMA AR	Tourism demand Economic variables	Forecasting performance is highly dependent on the forecasting horizon; Explanatory variable did not improve the performance;
[72]	M	ARIMA MSS	Tourism demand Economic variables	ARIMA outperformed the multivariate state space model consistently;
[2]	Q	MA	Tourism demand	Moving-Average is suitable for separating the seasonal component but not for forecasting;
[7]	M	SARIMA, HEGY test, HW, LR	Tourism demand	SARIMA with HEGY test outperformed the Holt-Winters and linear regression;

Note: extreme learning machine (ELM) model; kernel extreme learning machine (KELM) model; artificial neural network (ANN) model; support vector regression (SVR); least square support vector regression (LSSVR); autoregressive moving average (ARMA); autoregressive integrated moving average (ARIMA); autoregressive fractionally integrated moving average (ARFIMA); logistic regression (LR) model; historical average (HA) model; vector autoregressive (VAR) model; bayesian global vector autoregressive (BGVAR) model; multiseries structural time series (M-STSM) model; multivariate singular spectrum analysis (MSS); singular spectrum analysis (SSA); exponential smoothing (ETS); generalized dynamic factor model (GDFM); principle component analysis (PCA); autoregressive fractionally integrated moving average model with exogenous inputs model (ARIMAX); FOA algorithm for three parameters selection of the SVR model with seasonal adjustment (SFOASVR); dynamic linear model (DLM); Holt-Winter (HW); seasonal naïve (SNAIVE); autoregressive distributed lag model (ADLM); autoregressive distributed lag model (ADLM); error-correction ADLM (EC-ADLM); autoregressive mixed-data sampling (AR-MIDAS); tourism demand forecasting system (TDFS); Modular Genetic-Fuzzy Forecasting System (MGFFS); empirical mode decomposition (EMD); back-propagation neural network (BPNN); time-varying parameter structural time series model (TVP-STSM); autoregressive distributed lag models (ADLM); state space models (SS); dynamic econometric (DE); error correction model (ECM); variance covariance (VC); Hylleberg-Engle-Granger-Yoo Test (HEGY test); winter model (WM); multivariate state space (MSS); moving-average (MA); Holt-Winters (HW); sine wave (SW);

Appendix Table 8 Overview of studies related to machine learning-based tourism forecasting and published in the last decade; the frequency of data is provided per week (W), per month (M), quarterly (Q) and per year. Traditional econometrics models have also been included as benchmark models.

Paper	Data Freq.	Methodology	variables	Finding and Limitation
[73]	M	SAE, ESN	Tourist demand, search query	SAE with ESN model with search query outperforms SARIMA, SVR, and LSTM.
[20]	M	ARIMA, ETS, ANN, TBATS, ARFIMA, SSA, MA	Tourist arrivals,	No single model outperformed all others consistently; SSA-R, SSA-V, ARIMA, and TBATS models are better than others;
[19]	M	ARIMA SETAR ANN	Tourist arrivals,	ARIMA outperformed SETAR and ANN for short horizons; Optimized structure with pre-processing of the data may improve the ANN performance;
[74]	Q	SVR, GA	Tourist demand	SVR with GA outperform other benchmark models;
[15]	Q	STSM, ANN, Naïve, HW	Tourist arrivals	Basic structural method (BSM) achieved the best performance; ANN, if structured correctly, can outperform BSM significantly;
[18]	M	ANN, GA, ARIMA, ETS, MA, Naïve	Tourist arrivals	ANN outperformed all other models in forecasting tourist arrivals to Durban from US; Time-series analysis is valuable for tourism forecasting;

[17]	M	BNN LR, TS, FNN	Tourist arrivals, Service Price, Hotel rate, FX, Number of visitors, Marketing Expenses, Gross Domestic Expenditure	Back-propagation NN captured the non-linearity of the tourist arrivals better than all other benchmark models; Feed-forward NN performed the worst;
[75]	Annual	ANN, MR, Naïve, MA, ETS	Tourist arrivals, Service Price, Hotel rate, FX, Population, Marketing Expenses, Gross Domestic Expenditure	ANN outperformed all benchmark models in forecasting Japaness tourist arrivals
[16]	Q	ANN, MR	Tourist arrivals, Economic variables	ANN outperformed multi-regression in forecasting tourist arrival;

Note: stacked autoencoders (SAE); recurrent neural network (ESN) artificial neural network (ANN) model; support vector regression (SVR); Genetic Algorithm (GA); singular spectrum analysis (SSA); self-exciting threshold autoregressions (SETAR); genetic algorithm (GA); Back-propagation neural network (BNN); time-series model (TS); Feed-forward neural network (FNN); Multiple regression (MR);